Molecular Pharmacology Fast Forward. Published on July 15, 2008 as doi: 10.1124/mol.108.049676
This article has not been copyedited and formatted. The final version may differ from this version.

Structural motifs of importance for the constitutive activity of the orphan 7TM receptor EBI2 – Analysis of receptor activation in the absence of an agonist.

Tau Benned-Jensen and Mette M. Rosenkilde

Laboratory for Molecular Pharmacology, Department of Neuroscience and Pharmacology, Faculty of Health Sciences, The Panum Institute, Copenhagen University, Blegdamsvej 3, 2200-Copenhagen, Denmark.

Molecular Pharmacology Fast Forward. Published on July 15, 2008 as DOI: 10.1124/mol.108.049676
This article has not been copyedited and formatted. The final version may differ from this version.

a) Running title: *ArgII:20 in TM-2 is important for EBI2 receptor activation.*

b) Address correspondence to:

Mette M. Rosenkilde, Laboratory for Molecular Pharmacology,

Department of Neuroscience and Pharmacology, The Panum Institute,

Copenhagen University, Blegdamsvej 2, 2200 Copenhagen, Denmark,

Phone: 0045 61364871, Fax: 0045 35327610, e-mail: rosenkilde@sund.ku.dk

c) Number of text pages: 23

Number of tables: 2,

Number of figures: 9, plus 3 supplemental figures

Number of references: 40

Number of words in *Abstract*: 250

Number of words in *Introduction*: 750

Number of words in *Discussion*: 1499

d) List of non-standard abbreviations: 7TM, seven transmembrane spanning receptors; EBI2, Epstein-Barr Induced receptor 2; EBV, Epstein-Barr virus; wt, wildtype; ECL2, extracellular loop 2; CB, cannabinoid; mGluR5, metabotropic Glutamate receptor 5;

Molecular Pharmacology Fast Forward. Published on July 15, 2008 as DOI: 10.1124/mol.108.049676
This article has not been copyedited and formatted. The final version may differ from this version.

Abstract

The Epstein-Barr induced receptor 2 (EBI2) is a lymphocyte-expressed orphan 7TM receptor, that signals constitutively through Gαi as shown for instance by GTPγS incorporation. Two regions of importance for the constitutive activity were identified by a systematic mutational analysis of 29 residues in EBI2. The CREB-transcription factor was used as a measure of receptor activity, and was correlated to the receptor surface expression. PheVI:13 (Phe^{257}), and the neighbouring CysVI:12 (Cys^{256}), in the conserved CW/FxP motif in TM-6, acted as negative regulators as Ala substitutions at these positions increased the constitutive activity 5.7 and 2.3 fold, respectively, compared to EBI2 wildtype (wt). In contrast, ArgII:20 (Arg^{87}) in TM-2 acted as a positive regulator, as substitution to Ala, but not to Lys, decreased the constitutive activity more than 7 fold compared to wt EBI2. IleIII:03 (Ile^{106}) is located only 4Å from ArgII:20, and a favourable electrostatic interaction with ArgII:20 was created by introduction of Glu in III:03 as the activity increased to 4.4 fold of wt EBI2. Importantly, swapping these charges by introduction of Glu in II:20 and Arg in III:03, resulted in a 2.7-fold increase compared to wt EBI2, and thereby rescued the two signaling-deficient single-mutations, that exhibited a 3.8- to 4.5-fold decrease in constitutive activity. The uncovering of these molecular mechanisms for EBI2 activation is important from a drug development point-of-view, as it may facilitate the rational design and development of small-molecule inverse agonists against EBI2 of putative importance as antiviral- or immune modulatory therapy.

Molecular Pharmacology Fast Forward. Published on July 15, 2008 as DOI: 10.1124/mol.108.049676
This article has not been copyedited and formatted. The final version may differ from this version.

G protein-coupled seven transmembrane α-helix-spanning receptors (7TM receptors) constitute one of the largest superfamilies of proteins in the human genome and are targets for >30% of all drugs on the market. The endogenous ligands are highly diverse and span from photons, metals, nucleotides, biogenic amines, amino acids, peptides and proteins, to lipids, steroids and Krebs-cycle intermediates. Approximately 750 7TM receptors have been identified in the human genome including ~350 olfactory and ~30 other chemosensory receptors. The non-olfactory and non-chemosensory receptors are divided into four families: Class A (rhodopsin-like), B, C, and F/S (Frizzled), of which Class A is by far the largest (284 members). The EBI2 receptor was identified in 1993 as one of the most upregulated genes in lymphocytes infected with Epstein-Barr virus (EBV, hence the name Epstein-Barr induced receptor 2, EBI2) (Birkenbach et al., 1993). It is expressed predominantly in lymphoid tissue and constitutes one of ~150 orphan receptors within Class A (Vassilatis et al., 2003). Despite this, it was recently described to signal with high constitutive activity through Gαi (Rosenkilde et al., 2006).

Constitutive activity is a well known phenomenon among 7TM receptors, and occurs within wildtype (wt) as well as mutated receptors, although is should be noted that *in vitro* observed constitutive activity could also result from artificial receptor over-expression (Seifert and Wenzel-Seifert, 2002). However, the fact that constitutive activity has been associated with multiple diseases, for instance retinitis pigmentosa (rhodopsin mutations), pigmentation defects (MSH receptor mutations), and hyperfunctional thyroid adenomas (TSH receptor mutations) (Parma et al., 1995;Robbins et al., 1993) support a biological relevance, at least in these receptors. Interestingly, constitutive activity is a hallmark for the majority of herpesvirus-encoded 7TM receptors, exemplified by the broadspectrum activity of ORF74 from Human Herpesvirus 8 (HHV8) and the selective constitutive activity through Gαi of the EBV-encoded BILF-1 receptor (Bais et al., 1998;Rosenkilde et al., 1999;Paulsen et al., 2005;Beisser et al., 2005). The >200-fold induction of EBI2 upon EBV cell entry is the only known modulation of EBI2 (Birkenbach et al., 1993), and the biologic function therefore remains to be described. Due to the orphan status, the only pharmacologic "handle" at present is the constitutive activity.

Molecular Pharmacology Fast Forward. Published on July 15, 2008 as DOI: 10.1124/mol.108.049676
This article has not been copyedited and formatted. The final version may differ from this version.

The molecular mechanism behind 7TM receptor activation has been a major area of research for many years, and was advanced by the crystal structure of bovine rhodopsin in 2000 (Palczewski et al., 2000) and the very recently published crystal structures of the β2-adrenergic receptor (Cherezov et al., 2007;Rasmussen et al., 2007). Based on these crystals and on mutational analysis with for example metal-ion site engineering and disulfide engineering or biophysical experiments in for example rhodopsin and the adrenergic receptors, a toggle switch model have been proposed in which the transmembrane helices move during receptor activation in a way that creates space for the G-protein and/or adaptor protein at the intracellular edge, whereas extracellular segments of the helices approach each other (Hubbell et al., 2003;Shi et al., 2002;Elling et al., 2006;Schwartz et al., 2006).

In the present study we focus on the molecular mechanism behind the constitutive activity of EBI2 (Fig. 1), and show in addition, that this activity can be measured as an increase in GTPγS-binding in EBI2 expressing lymphocytes and HEK-293 cells (Fig. 2). In contrast to most other rhodopsin-like receptors, EBI2 is not part of any larger subfamily (Vassilatis et al., 2003), and the closest human homolog is GPR18 to whom it only shares 23.1% homology and 40.2% similarity. Although EBI2 lacks obvious homology-partners, it still contains the conserved residues identified in most other rhodopsin-like 7TM receptors (Asn I:18[1], Asp II:10, Cys III:01, Trp IV:10, and the three Pro's in positions V:16, VI:15, and VII:17) (Fig. 1). We created 44 mutations in 29 residues located in the transmembrane helices based on the proposed models for receptor activation within Class A (Hubbell et al., 2003;Schwartz et al., 2006) (Fig. 1). The residues were chosen based on their prevalence in Class A, or based on being part of well-known functional motifs. Side-chain elimination with Ala-substitution was used most frequently. However, in certain cases we introduced residues with similar chemical properties (for instance Phe to Trp or Arg to Lys), changed charge (for instance Arg to Glu) or introduced size in a steric hindrance approach (for instance introduction of Trp). Consistent with the current models for receptor activation, we find that the CWxP motif in TM-6 (in EBI2 CFxP) regulates receptor activation, and in addition, we identify Arg^{87} (in position II:20) as being important for maintenance of the high constitutive activity of EBI2.

Molecular Pharmacology Fast Forward. Published on July 15, 2008 as DOI: 10.1124/mol.108.049676
This article has not been copyedited and formatted. The final version may differ from this version.

Materials and Methods

Materials. EBI2 was kindly provided by H.R. Luttichau, Laboratory for Molecular Pharmacology, and corresponded to the Genbank accession number L08177. The promiscuous chimeric G protein GαΔ6qi4myr (abbreviated Gqi4myr) was kindly provided by Evi Kostenis (Rheinische Friedrich-Wilhelm University, Bonn, Germany). Lipofectamine^{TM} 2000 reagent and OPTIMEM was purchased from Life Technologies. LucLite (Lyophilized Substrate Solution) was from Packard (Boston, MA). Goat anti-mouse horseradish peroxidase-conjugated antibody was from Pierce (Rockford, IL), while mouse anti-FLAG (M1) antibody, forskolin and pertussis toxin were from Sigma Chemicals Co. (St. Louis, MO). Both SlowFade Antifade reagent and goat anti-mouse Alexa Fluor 488-conjugated antibody were from Molecular Probes (Carlsbad, CA). The TMB (3,3',5,5'-tetramethylbenzidine) substrate was purchased from KemEnTech (Taastrup, Denmark).

Site-directed mutagenesis. All EBI2 constructs were inserted into a modified pcDNA3 vector, kindly provided by Kate Hansen (7TM-Pharma, Denmark), which contained an upstream sequence encoding a hemagglutinin signal peptide fused to the FLAG tag. Site-directed mutagenesis was carried out using the *Pfu* polymerase (Stratagene) and the generated mutations were verified by bidirectional DNA sequencing at MWG Biotech (Martinsried, Germany).

Transfection and tissue culture. HEK293 cells were grown in DMEM adjusted to contain 4500 mg/L glucose (Invitrogen, Cat. No 31966-021), 10% FBS (fetal bovine serum), 180 u/ml penicillin and 45 ug/mL streptomycin (PenStrep) at 10% CO_2 and 37ºC. Stably transfected HEK293 cells were grown in the same medium but with G418 added at 800 mg/mL as was stably transfected TREX-HEK293 cells but with blasticidin and Zeocin (both Invitrogen) added at 5 and 100 μg/mL, respectively. L1.2 pre-B cells were grown in RPMI supplemented with 10% FBS, PenStrep and G418 at 800 mg/mL. For transient transfections, the Lipofectamine^{TM} 2000 reagent in the serum-free medium OPTIMEM was used according to the manufacturer's description. Briefly, the cells were transfected for 5 hours at 37 ^{o}C using Lipofectamine^{TM} 2000 at 12 μL/ml and DNA at varying concentrations and subsequently incubated in fresh growth medium

Molecular Pharmacology Fast Forward. Published on July 15, 2008 as DOI: 10.1124/mol.108.049676
This article has not been copyedited and formatted. The final version may differ from this version.

for 48 hours before usage. Cells were always transfected in parallel for the CREB luciferase and ELISA assays. HEK293 and TREX-HEK293 clones stably expressing FLAG-tagged wt EBI2 were generated by transfecting the cells with FLAG-tagged wt EBI2 cloned into pcDNA3.1 or pcDNA4/TO, respectively, and selected using G418 or Zeocin. The L1.2 pre-B cell line stably expressing a wt EBI2-GFP fusion protein was generated as previously described (Rosenkilde et al., 2006).

Membrane preparation. Membranes were prepared from naïve HEK293 cells, HEK293 cells stably expressing FLAG-tagged wt EBI2, naïve L1.2 pre-B-cells, L1.2. cells stably expressing C-terminally GFP-tagged wt EBI2 and induced or uninduced TREX-HEK293 stably transfected with FLAG-tagged wt EBI2. In the latter case, the expression of the receptor was induced by incubating the cells in growth medium containing 5 ng/mL doxycycline (Invitrogen) for 48 hours. The cells were manually harvested with a rubber policeman in ice cold PBS and homogenized using a Dounce on ice. The homogenate was centrifuged at 500 rpm for 3 min at 4 ^{o}C. Subsequently, the supernatants were collected and centrifuged at 20000 rpm at 4 ^{o}C. The resulting membrane pellets were resuspended in 20 mM HEPES buffer containing 2 mM $MgCl_2$ and Complete protease inhibitor mixture (Roche, Mannheim, Germany) and kept at -80 ^{o}C until subjected to [^{35}S]GTPγS binding experiments. The protein concentrations in each preparation were determined using the BCA protein assay kit (Pierce).

[^{35}S]GTPγS binding assay. [^{35}S]GTPγS binding experiments were carried out in white 96-well plates (Nunc) using the SPA-based method. A volume of membrane preparation (corresponding to 20 μg protein/well) were diluted in assay buffer (final concentrations: 50 mM HEPES, 2 mM $MgCl_2$, 50 mM NaCl, 1 mM EGTA, 1 μM GDP, 0.1% BSA and Complete inhibitor mix). [^{35}S]GTPγS (Perkin Elmer, 1250 Ci/mmol, 12.5 mCi/mL) diluted in assay buffer was added to a final concentration of 1 nM and incubated 30 min at room temperature. Subsequently, WGA-coupled SPA-beads (Amersham Biosciences) was added (final concentration of 2.8 mg/mL) followed by 30 min incubation at room temperature on a plate shaker. Finally, the plates were centrifuged at 1500 rpm for 5 min and the amount of radioactivity determined using a Top

Molecular Pharmacology Fast Forward. Published on July 15, 2008 as DOI: 10.1124/mol.108.049676
This article has not been copyedited and formatted. The final version may differ from this version.

Count scintillation counter (Packard Instruments). The level of unspecific binding was determined by adding unlabelled GTPγS at a final concentration of 40 μM.

CREB trans-reporting luciferase assay. The signaling was determined using the trans-reporting CREB-luciferase assay according to the manufacturer's recommendations (Stratagene, La Jolla, USA). Cells were seeded at 80.000 cells/well in 96-well culture plates 24 h prior to transfection and were transfected with the trans-activator plasmid pFA2-CREB and the reporter plasmid pFRLUC at 6 ng/80.000 cells (i.e. 6 ng/well) and 50 ng/80.000 cells (i.e. 50 ng/well), respectively. In most experiments (Fig. 3-7), the cells were co-transfected with the chimeric G-protein, GαΔ6qi4myr (abbreviated as Gqi4myr) at 30 ng/80.000 cells, (Kostenis, 2002). However, as a more direct measurement of cAMP inhibition, forskolin (15 uM) was added in stead of Gqi4myr, and the effect of increasing concentrations of receptor DNA on cAMP-induced CREB-activation was measured (Fig. 9) in the absence or presence of pertussisn toxin (100 ng/ml). The CREB activity was determined 48 h after transfections using the LucLite substrate (Perkin Elmer). Briefly, the cells were washed twice in Dulbecco's PBS (0.9 mM $CaCl_2$, 2.7 mM KCl, 1.5 mM KH_2PO_4, 0.5 mM $MgCl_2$, 137 mM NaCl, and 8.1 mM Na_2HPO_4) and the luminescence was measured in a micro plate scintillation and luminescence counter (Top-counter, Packard) after 10 min. incubation in 100 μL Dulbecco's PBS and 100 μL Luc-Lite substrate. Every receptor construct were tested in parallel with EBI2 wt receptor at least thrice in quadruples.

Enzyme-Linked Immunosorbent Assay (ELISA). HEK293 cells were transiently transfected with the indicated FLAG-tagged EBI2 constructs using Lipofectamine™ 2000 as described above. Forty-eight hours after transfection the cells were fixed in 4% glutaraldehyde for 10 min, washed thrice in TBS and blocked for 30 min with TBS containing 2% BSA. Subsequently, the cells were incubated with mouse anti-FLAG M1 antibody at 2 ug/ml for 2 h in TBS supplemented with 1% BSA and 1 mM $CaCl_2$. After three washes in TBS containing 1% BSA and 1 mM $CaCl_2$, the cells were incubated for 1 h with goat anti-mouse horseradish peroxidase-conjugated antibody diluted 1:1000 in the same buffer as the primary antibody. Following

Molecular Pharmacology Fast Forward. Published on July 15, 2008 as DOI: 10.1124/mol.108.049676
This article has not been copyedited and formatted. The final version may differ from this version.

washing, the immune reactivity was determined by addition of TMB according to manufacturer's instruction. All steps were carried out at room temperature.

Data handling. The relative constitutive activity, given as mean ± SEM in fold compared to wt, is calculated by normalizing the CREB signaling (CS) to cell surface expression (SE) as measured by ELISA according to:

(1) $Constitutive\ activity = CA = \frac{CS}{SE}$ and (2) $CA_{mut,relative} = \frac{CA_{mut}}{CA_{wt}} = \frac{CS_{mut} \cdot SE_{wt}}{SE_{mut} \cdot CS_{wt}}$

Statistic analysis. All statistic analyses were performed as the Student's t tests.

Immunocytochemistry. HEK293 cells were seeded on poly-L-lysine-coated coverslips in 6-well plates at $5 \cdot 10^5$ pr well. The following day the cells were transfected with the indicated FLAG-tagged EBI2 constructs at 150 ng/well using Lipofectamine™ 2000 as described above. Forty-eight hours after transfection the specimens were fixed in 4% paraformaldehyde for 15 min, washed thrice in TBS and blocked for 20 min with TBS (0.05 M Tris Base, 0.9 % NaCl, pH 7.6) containing 2% BSA. Receptors residing at the cell surface were labelled by incubation with mouse anti-FLAG M1 antibody at 2 µg/mL in TBS containing 1% BSA and 1 mM $CaCl_2$ for 1 h. After three washes with TBS containing 1 mM $CaCl_2$, labelled receptors were detected by incubating with goat anti-mouse Alexa Fluor 488-conjugated IgG antibody diluted 1:1000 in TBS containing 1% BSA and 1 mM $CaCl_2$ for 30 min. Subsequent to washing, the specimens were mounted in SlowFade Antifade reagent using nail polish as sealing. Mock transfected cells were included to ensure no unspecific binding of either primary or secondary antibodies. All steps were performed at room temperature.

Confocal microscopy. Confocal microscopy was performed using a LSM 510 laser scanning unit coupled to an inverted microscope with a 63x 1.4 numerical aperture oil immersion Plan-Apochromat objective (Carl Zeiss). Alexa-Fluor 488 was excited using an argon-krypton laser (λ = 488 nm) and the emission collected

Molecular Pharmacology Fast Forward. Published on July 15, 2008 as DOI: 10.1124/mol.108.049676
This article has not been copyedited and formatted. The final version may differ from this version.

with a 505 nm long-pass filter. Images were recorded in 1024 x 1024 pixels and averaged over 16 whole frame scans.

Molecular Pharmacology Fast Forward. Published on July 15, 2008 as DOI: 10.1124/mol.108.049676
This article has not been copyedited and formatted. The final version may differ from this version.

Results

Constitutive activity of wt EBI2 through GTPγS binding. One of the most widely used methods to determine receptor activation of G-proteins is the measurement of [^{35}S]-GTPγS binding. The previously shown constitutive activity of EBI2 through Gαi (Rosenkilde et al., 2006) (as summarized Fig. 2A and B) was supported by a significant increase in [^{35}S]-GTPγS binding in membranes from HEK-293 cells stably expressing EBI2, or expressing EBI2 under the tetracyclin-inducible promoter (TREX-system) compared to naïve HEK293 cells or uninduced EBI2 TREX-HEK293 cells. (Fig. 2C). This was also shown in membranes from L1.2 lymphocytes stably expressing EBI2 fused with GFP (Fig. 2D). In all cases, the receptor was well expressed at the surface as demonstrated by ELISA (HEK293) or confocal microscopy (L1.2) (data not shown).

Structural motifs of importance for the constitutive activity. No endogenous or exogenous ligands have yet been identified for EBI2. We therefore normalized the signaling activity to surface expression in order to compare mutations with each other. Consequently, all mutations were created with an N-terminal M1 FLAG tag, which did not affect EBI2 signaling (Rosenkilde et al., 2006), and the cell-surface expression was quantified in HEK293 cells transiently transfected with 0, 15 and 25 ng receptor DNA by an ELISA-technique using the M1 anti-FLAG antibody as primary and the horseradish peroxidise-conjugated antibody as secondary antibody. The constitutive activity through Gαi was measured in HEK293 cells as the activation of the transcription factor CREB in the presence of Gqi4myr (a chimeric Gα-subunit that is recognized by Gαi coupled receptors, but activates Gαq regulated downstream pathways) (Kostenis, 2002) at four receptor concentrations (0, 5, 15, and 25 ng/80.000 cells). For all mutations the relative constitutive activity was determined by correlating the activity to the surface expression at 15 and 25 ng receptor DNA/80.000 cells (Tables 1 and 2).

TM-6 is involved in the regulation of constitutive activity. The motif including the conserved Pro in TM-6 (CFxP in EBI2) was changed into the most frequently occurring CWxP-motif by mutating PheVI:13 (Phe^{257})

Molecular Pharmacology Fast Forward. Published on July 15, 2008 as DOI: 10.1124/mol.108.049676
This article has not been copyedited and formatted. The final version may differ from this version.

to Trp, F(VI:13)W-EBI2. Interestingly, this substitution had no effect on the constitutive activity of EBI2 (Fig. 3A, Table 1). In contrast, introduction of Ala substantially increased the activity 5-6 fold, and introducing a polar residue (Cys) resulted in a similar increase (3-4 fold) (Fig. 3A, Table 1). Contrary to the Trp introduction that only slightly decreased the surface expression (to 73% of wt EBI2), a huge decrease was observed for the Ala and Cys introductions (7 and 17% of wt EBI2) (Fig. 3C, Table 1). Despite this, these receptors could still be observed on the surface by confocal microscopy using an antibody against the N-terminal Flag-tag and a secondary Alexa Fluor 488-conjugated antibody (Fig. 3D-F).

Linearity is a prerequisite for the correlation of receptor activity with surface expression. Therefore, prior to the mutational screening, we performed 12-point gene-dose experiments ranging from 1 ng to 35 ng of wt EBI2 receptor per 80.000 cells and determined receptor activity as well as surface expression for all doses. As seen in Fig. 4A, there was an almost linear correlation (r^2=0.94) between receptor activity and surface expression within the chosen DNA concentrations (see supplemental Fig. 1A and B for the corresponding CREB-activity and expression measurements, respectively). However, at very low (1 ng/80.000 cells) and very high (30-35 ng/80.000 cells) DNA concentrations a tendency of lower activity per expressed molecule was observed. This could be due to a higher threshold for the measurement of activation compared to surface expression for the low DNA concentration, and a saturation of the CREB-activation pathway for the high DNA concentrations. However, between 5 and 25 ng receptor DNA we observed a linearity that validated the correlation of receptor activity with surface expression within these concentrations. As the increases in relative activity for the Ala and Cys introductions in VI:13 were mainly determined by a very low receptor expression (Fig. 3A-C), we included multiple gene-doses (see supplemental Fig. 2) for F(VI:13)A- and F(VI:13)C-EBI2 and adjusted to exactly the same expression level as wt EBI2. For identical expression-levels (white bars Fig. 4B), a similar increase in activity appeared (black bars Fig. 4B) as obtained from the correlation of expression and activity for fixed DNA concentrations (Table 1, Fig. 3A).

Impact of aromatic residues in TM-5 and -6 in the vicinity of PheVI:13 on EBI2 signaling. The aromatic environment surrounding VI:13 in the major binding pocket[2] is important for agonist-dependent, as

Molecular Pharmacology Fast Forward. Published on July 15, 2008 as DOI: 10.1124/mol.108.049676
This article has not been copyedited and formatted. The final version may differ from this version.

well as constitutive activity in many receptors (see discussion). In TM-5, position V:13 is highly conserved as an aromatic residue being either Phe (70%) or Tyr (11%) as in EBI2 and has been suggested to be part of an aromatic cluster of importance for receptor activity (Schwartz et al., 2006). In EBI2, however, only a 1.4-fold reduction in constitutive activity compared to wt activity was obtained upon substitution of Tyr^{205} to Ala, whereas introduction of Phe resulted in a modest increase in the relative activity of 1.4-fold (Table 1). In TM-6, two other highly conserved aromatic residue important for activity in some receptors (see discussion) are found in the vicinity of PheVI:13, namely TyrVI:16 and PheVI:09 located one helical turn above and below, respectively (Fig. 1B). However, no effect was observed for F(VI:09)A-EBI2 (Fig. 5A-C, Table 1). In contrast, an Ala-substitution of TyrVI:16 resulted in a decrease in relative constitutive activity of 2.3-fold. A similar decrease (1.9-fold) was obtained by introducing Phe at this position (Fig. 5A-C, Table 1), indicating that the hydroxyl group influences receptor activity.

CysVI:12 has been suggested to act in concert with the aromatic residue in position VI:13 in the β2-adrenergic receptor (that holds a Trp in VI:13) (Shi et al., 2002). We therefore substituted it to Ala and interestingly observed a large increase in the constitutive activity (2.3-fold relative to wt EBI2) (Table 1). MetVI:24 is another residue of note in TM-6 as this position very seldom (only in 2%) holds a Met. We therefore introduced an Ala (the most common amino acid at this position) and observed no change in the activity or expression, i.e. no change in the relative constitutive activity (Table 1).

Impact of residues in TM-3, -5 and -7 facing into the major binding pocket on receptor activation. Biophysical evidence indicates that TM-7 and TM-3 move in concert with TM-6 during receptor activation (Farrens et al., 1996). We therefore substituted a total of 6 residues in the extracellular segments of these two helices pointing towards the major binding pocket (PheIII:08 and ThrIII:12 in TM-3 and ThrVII:05, ValVII:06, MetVII:09, and AsnVII:12 in TM-7). Collectively, these 6 Ala mutations had no major impact (a factor of <1.5) on the relative constitutive activity (Table 1). In more detail, the residue in III:08 is often an aromatic (23%) and as such part of the aromatic cluster (see Discussion). However, in EBI2, an Ala in III:08 only slightly decreased the activity (1.3-fold), whereas introduction of Tyr resulted in an 1.9-fold increase

Molecular Pharmacology Fast Forward. Published on July 15, 2008 as DOI: 10.1124/mol.108.049676
This article has not been copyedited and formatted. The final version may differ from this version.

compared to wt EBI2 (Table 1). Met infrequently occurs at position VII:09 (1%) which usually contains Ala (40%) or Gly (20%). Nevertheless, substitution to Ala only resulted in a minor decrease in constitutive activity (1.4-fold), while introduction of Phe resulted in a minor increase in relative constitutive activity (to 1.1-fold, Fig. 5D-F). Similarly, introduction of Ala in position VII:06 resulted in a minor increase in the relative constitutive activity (1.3-fold of wt EBI2) (Fig. 5D). The expression levels of these mutations in VII:06 and VII:09 were similar to wt EBI2 (Fig. 5F).

In contrast to TM-3, -6, and -7, the role of TM-5 in receptor activation is poorly defined, although position V:13 may have an important role in some receptors (see above). Position V:12, that protrudes right into the major binding pocket, is conserved as a small amino acid (Gly in 29% and Leu in 14%), and in some receptors introduction of larger side-chains abolishes receptor activity (unpublished observation Pia Cwarzko Jensen, Stefanie Thiele and Mette M. Rosenkilde). Despite this, we only observed a minor decrease (1.6-fold) for the substitution of Gly for Trp in V:12 (Table 1). A similar minor effect was observed for the exchange of Cys in position V:09 (which holds a Cys in only 4%) to Ala (Table 1).

ArgII:20 is important for the constitutive activity of EBI2. Emerging evidence suggests that residues pointing into the *minor* binding pocket or residues located elsewhere in the helices confining the minor binding pocket (TM-1, -2, -3, and -7) are also important for receptor activation (Zhou et al., 1994;Miura and Karnik, 2002;Govaerts et al., 2001a;Govaerts et al., 2003;Rosenkilde et al., 1994). Position II:20 usually contains an aromatic residue (31%) or a Leu (20%), and only seldom an Arg (7%) or a Lys (4%) (Mirzadegan et al., 2003). Upon introduction of an Ala in II:20 we observed a substantial decrease (11-fold) in the measured CREB-activity (Fig. 6B) and a 1.4-fold decrease in surface expression (Fig. 6C). The relative constitutive activity for this mutation was therefore decreased 7.1-fold relative to wt (Fig. 6A). In contrast, introduction of a charge-conserving Lys had no impact on the activity, while introduction of a charge-reversing Glu resulted in a major reduction in activity (3.8-fold) compared to wt EBI2 (Fig. 6A). Three other residues on the same side of TM-2 were also mutated into Ala (LeuII:17 and PheII:13 located one and two helical turns below ArgII:20, respectively, and TyrII:24 located one helical turn above) with no

Molecular Pharmacology Fast Forward. Published on July 15, 2008 as DOI: 10.1124/mol.108.049676
This article has not been copyedited and formatted. The final version may differ from this version.

effect on the activity of EBI2 (Table 2). This clearly indicates that charge is important, and that ArgII:20 does not act in concert with any other residues in TM-2 for the maintenance of high constitutive activity. In contrast to the mutations in TM-6 (Fig. 3C, -5C, Table 1), there were no major changes in receptor surface expression for the mutations in TM-2 (Fig. 6C, Table 2).

Putative ArgII:20 electrostatic partners: anionic EC loop-2 (ECL2) residues. No obvious electrostatic partners for ArgII:20 are present at the same horizontal level in EBI2 (Fig. 1A). However, in ECL2, which is constrained in close proximity to the membrane surface through a disulfide-bridge to the conserved CysIII:01, a total of 5 Glu residues are present (Fig. 1A). Glu^{183} is located closest to Cys^{181} in ECL2 (that forms the disulfide-bridge to CysIII:01), and was therefore substituted to Ala, (E183A)-EBI2. Although this mutation resulted in a 1.3-fold decrease in the relative constitutive activity, this was clearly not even approaching the impact of ArgII:20. Furthermore, the four additional anionic amino acids located either prior to Cys^{181} (Glu^{175} and Glu^{177}) or after (Glu^{188} and Glu^{189}) were substituted to Ala in a pair wise manner with no decrease in the constitutive activity of EBI2 (Table 2). In fact, a minor increase was observed for the (E188A;E189A)-EBI2 mutation (1.3-fold compared to wt EBI2). Consequently, the two double mutants were combined with (E183A)-EBI2 creating the two triple-mutants (E175A;E177A;E183)-EBI2 and (E183A;E188A;E189A)-EBI2. The former had the same minor effect as (E183A)-EBI2 (1.4-fold decrease in activity), whereas the triple mutant incorporating the three Glu residues after Cys^{181}, resulted in a 1.8-fold decrease, Table 2. All in all, these substitutions indicate that the Glu residues in ECL2 do not act in concert as anionic partners with ArgII20 (Table 2) (Fig. 6A).

Putative ArgII:20 hydrogen-bond interaction partners: residues in TM-3 and -7. Due to the rather inconclusive results in identifying anionic partners, we searched for possible hydrogen-bond interacting partners in TM-3, and -7 for ArgII:20. In TM-7, AsnVII:10 (Asn^{298}) has the chemical properties and proper horizontal locality to make hydrogen-bonds with ArgII:20, and is in fact infrequently occurring at this position (1%). However, Ala introduction in VII:10 had no impact on the constitutive activity (Table 2). Two additional residues in TM-7 with hydrogen-bonding capabilities, HisVII:03 (His^{293}) and CysVII:14 (Cys^{302}),

Molecular Pharmacology Fast Forward. Published on July 15, 2008 as DOI: 10.1124/mol.108.049676
This article has not been copyedited and formatted. The final version may differ from this version.

were mutated to Ala, yet again with no impact on the activity of EBI2 (Table 2). In TM-3, ThrIII:04 is pointing toward TM-7 and TM-2, and is capable of hydrogen-bonding. However, no effect was observed upon introduction of Ala (Table 2). In contrast, introduction of Glu in III:04 (in an attempt to force TM-3 closer to ArgII:20 through a salt-bridge formation) resulted in a minor increase in activity (1.4-fold).

Beneficial effect of an electrostatic interaction between position II:20 and III:03. Due to the apparent beneficial effect of a Glu at position III:03, a model was built based upon the crystal structure of rhodopsin using SWISS-MODEL (swissmodel.expasy.org// SWISS-MODEL.html) and Deep Viewer v. 3.7 software, and residues in the proximity of ArgII:20 were identified by increasing the search radius from one to five Å in steps of 0.5 Å. Using this approach IleIII:03 appeared at a radius of 4Å, while ThrIII:04 appeared at 4.5Å. Consequently, IleIII:03 was mutated to Ala, Glu (as an attempt to introduce a salt-bridge to ArgII:20) and Arg (to create repulsion to ArgII:20) (Fig. 6D-F). Whereas the Ala introduction had no impact on EBI2 activity, the Glu introduction resulted in a major *increase* in constitutive activity (4.4-fold relative to wt EBI2) in contrast to a major decrease in case of the Arg in III:03 (4.6-fold) (Fig. 6D-F). These results together indicate a possible interaction between ArgII:20 and IleIII:03 as the introduction of Glu in III:03 $(+/-)^3$ increased the constitutive activity through a putatively formed salt-bridge, while the Arg introduction at III:03 (+/+) prevented activity through repulsion.

Exchange of charges in position II:20 and III:03. In order to substantiate the beneficial effect of the (+/-) electrostatic interactions (Fig. 6D), we swapped charges (-/+) by combining the two signaling-deficient single-mutations: R(II:20)E-EBI2 (-/0) and I(III:03)R-EBI2 (+/+) (Fig. 6A and 5D). The resulting double mutation (-/+) increased the constitutive activity 2.7-fold relative to wt (Fig. 7A), whereas as expected the double-mutant (-/-), created by Glu introductions at both positions, decreased the activity (Fig. 7A) (similar to (+/+), Fig. 6D). In contrast to the almost unaltered surface expression for the mutations of ArgII:20 (Fig. 6C), we observed a huge decrease for the mutations of III:03, especially for the Glu- and Arg-introduction (6.0% and 19% of wt EBI2 expression, respectively) (Fig. 6F). The double mutations obtained by combining these two mutations with the Glu-substitution of II:20 were expectedly equally low expressed (6.2 and 7.1%

Molecular Pharmacology Fast Forward. Published on July 15, 2008 as DOI: 10.1124/mol.108.049676
This article has not been copyedited and formatted. The final version may differ from this version.

of wt EBI2, Fig. 7C). However, despite this, confocal microscopy uncovered visible and reliable surface expression for all four mutations (Fig. 7D-G), and adjustment to exactly the same surface expression by varying the DNA concentrations revealed the same phenotype for the mutations in III:03 (suppl. Fig. 3). Thus as summarized in Fig. 8, these data strongly suggest that the constitutive activity of EBI2 can be regulated through an interaction between II:20 and III:03, since the single-mutation with Glu-introduction in III:03 (+/-) resulted in a 4.5-fold increase in constitutive activity (through electrostatic interactions with Arg II:20) and that these charges could be swapped (-/+) upon introduction of Glu in II:20 and Arg in III:03 (-/+). Importantly, the latter double-mutation (-/+) rescued the activity (>10-fold) of the corresponding signaling-deficient single-mutations (-/0) and (+/+), that exhibited a 3.8- to 4.5-fold decrease in activity compared to wt EBI2 to a 2.7-fold increase in the relative constitutive activity relative to wt (Fig. 8). Thus, the charge "swapping" (+/-) to (-/+) resulted in an increase in constitutive to almost the same levels as the (+/-). The difference in activity between (+/-) and (-/+) is probably due to the impact of ArgII:20 (Fig. 6).

Impact of ArgII:20 on Gαi coupling in the absence of the promiscuous G-protein. An additional approach was used to illustrate the impact of ArgII:20, namely measurements of receptor mediated inhibition of forskolin-induced cAMP production. The transcription factor CREB was used as a readout for the cAMP-levels in HEK-293 cells (Fig. 9A-D), and the receptor expression was determined in parallel (Fig. 9E and F). As seen in Fig. 9A, increasing concentrations of EBI2 DNA (0, 5, 15, and 25 ng/80.000 cells) inhibited forskolin-induced cAMP-production in a gene-dose dependent manner, and addition of pertussis toxin totally abolished this effect (as expected from the Gαi nature of EBI2 signaling) (Fig. 9A). The charge-conserved substitution of ArgII:20 to Lys had no impact on the signaling, while introduction of Ala and Glu impaired EBI2 signaling (Fig. 9B). None of the mutations in position II:20 had any huge impact on receptor expression. Introduction of Arg in position III:03 (+/+) impaired EBI2 signaling (charge-repulsion), while a Glu at this position (I(III:03)E (+/-) increased the signaling to wt levels (Fig. 9C). Given the very low expression of (I(III:03)E compared to wt (12% of wt, Fig. 9F), the relative activity for this construct was above wt levels (as observed in Fig. 6D). The charge-swapping mutation R(II:20)E;I(III:03)R (-/+) (Fig. 9D) increased the activity of the two signaling-defient R(II:20)E (-/0) (Fig. 9B) and I(III:03)R (+/+) (Fig.

Molecular Pharmacology Fast Forward. Published on July 15, 2008 as DOI: 10.1124/mol.108.049676
This article has not been copyedited and formatted. The final version may differ from this version.

9C), and given the low expression (6% of wt), the relative activity for this construct was above wt levels (as observed in Fig. 7A). Thus, the impact of ArgII:20, and the beneficial effect of (+/-) and (-/+) obtained by measuring cAMP-levels in HEK-293 cells (Fig. 9) were similar to the results obtained using the co-transfection with the promiscuous Gqi4myr (Fig. 6-7).

Molecular Pharmacology Fast Forward. Published on July 15, 2008 as DOI: 10.1124/mol.108.049676
This article has not been copyedited and formatted. The final version may differ from this version.

Discussion

The present study focuses on the molecular mechanism behind the constitutive activity of EBI2. As EBI2 lacks a known ligand, the receptor activity was normalized for surface expression. We analyzed 44 mutations in 29 residues broadly distributed around the major and minor binding pockets and in ECL2, and identified two regions of importance for the constitutive activity. Thus, we found that the middle of TM-6 (CFxP-motif), more specifically PheVI:13, functions as a negative regulator of activity, while ArgII:20 functions in the opposite way.

Quantification of receptor activity in the absence of an agonist. Constitutive activity is usually correlated to the maximum agonist-induced stimulation (Holst et al., 2004;Jensen et al., 2007). In the absence of agonists, the receptor activity was correlated to cell surface expression determined by ELISA using antibodies against the M1-FLAG-tag (Fig. 3, 5-7) – a method also used in other studies (Govaerts et al., 2001b;Srinivasan et al., 2007). Among the multiple receptor DNA concentrations analyzed (Fig. 4A), we chose 15 and 25 ng/80.000 cells for the correlations. Certain mutations with major impact on receptor activity displayed very low surface expression (for example Ala and Cys in VI:13, Fig. 3C and Glu and Arg in III:03, Fig. 6C). However, adjusted to the same expression level we observed similar activity fluctuations as obtained for the fixed (15 and 25 ng/80.000 cells) DNA concentrations. Thus, for the two mutations in VI:13, the activity was increased 1.6-2.5 fold for equal receptor expression (Fig. 4B, and suppl. Fig. 2) compared to 3-6 fold obtained from fixed DNA concentrations (Fig. 3A, Table 1). Similarly, introduction of Glu in III:03 resulted in a 1.5-2 fold increase while Arg decreased the activity 5-fold (suppl. Fig. 3), compared to the 4-fold increase and 5-fold decrease obtained for fixed DNA concentrations (Fig. 6D, Table 2).

The role of TM-6 and nearby residues for 7TM receptor activation. Movements of TM-6, and to a lesser extent TM-3 and -7, are essential for receptor activation (Farrens et al., 1996;Kim et al., 2004). The CWxP-motif in TM-6 has been identified as a key-regulator of movements with the Trp-residue acting as a rotameric toggle switch (Schwartz et al., 2006) - putatively in concert with CysVI:12 as suggested for the

Molecular Pharmacology Fast Forward. Published on July 15, 2008 as DOI: 10.1124/mol.108.049676
This article has not been copyedited and formatted. The final version may differ from this version.

β2-adrenergic receptor (Shi et al., 2002), or in concert with PheIII:12, as suggested for the cannabinoid CB1 receptor (McAllister et al., 2004). Thus, in many receptors, substitution of the aromatic residue in VI:13 results in abolished activity, for example in the amidergic receptors (Shi et al., 2002), the ghrelin receptor (Holst et al., 2004) and the CaSR (Ca^{2+}-sensing receptor) (Petrel et al., 2003). Position VI:13 in EBI2 contains a Phe that was exchangeable with Trp with no change in constitutive activity (Fig. 3A) and our finding of Phe/TrpVI:13 as a negative regulator (Fig. 3A, Table 1) is in clear contrast to these studies; however, several other 7TM receptors have shown the same phenotype as EBI2. For example, in the bradykinin receptor, a Gln substitution of TrpVI:13 creates constitutive activity (Marie et al., 1999), as does an Ala substitution in CCR8 (Jensen et al., 2007). Furthermore, Trp to Ala substitutions result in increased binding or action of agonists or positive allosteric modulators, for example in the CB1 receptor (McAllister et al., 2004), in the CXCR3 receptor (Rosenkilde et al., 2007) and in Class C mGluR5 (Muhlemann et al., 2006).

Position VI:13 is part of the aromatic cluster including residues in TM-3, -5, -6, and -7 (e.g. III:08 and -12, V:13, VI:16, VII:06 and -09) with importance for signaling in receptors regulated predominantly by small endogenous ligands (Roth et al., 1997;Shi et al., 2002;Holst et al., 2004;McAllister et al., 2004;Schwartz et al., 2006). However, in EBI2, we observed only minor decreases in the activity (1.4-2 fold compared to wt) for the Ala substitutions of PheIII:08, TyrV:13, and TyrVI:16, indicating that these aromatic side-chains play only minor roles, at least individually (Table 1). An interesting observation for these three residues was the rank-order of impact being Tyr>Phe>Ala for positions III:08 and VI:16, and Phe>Tyr>Ala for VI:13, indicating that hydrophobicity in addition to polarity matters at these positions. The slight increase in activity for the Met substitution to Phe in VII:09 is consistent with the impact of PheVII:09 (as part of the aromatic cluster) in the ghrelin receptor (Schwartz et al., 2006) and interestingly, the increased activity observed for the Ala substitution of CysVI:12 has also been observed in the β2-adrenergic receptor upon introduction of Thr for CysV:12 (Shi et al., 2002).

Molecular Pharmacology Fast Forward. Published on July 15, 2008 as DOI: 10.1124/mol.108.049676
This article has not been copyedited and formatted. The final version may differ from this version.

ArgII:20 – a major regulatory switch for the activity of EBI2. In general, TM-2 is not considered important for 7TM receptor activation, and in fact, not much attention has been paid to helices confining the minor binding pocket (TM-1,-2,-3, and -7). However, our data suggest otherwise (Fig. 4-9). Especially the beneficial effect of introducing electrostatic interactions between ArgII:20 (in wt EBI2) and Glu in III:03 (+/-), and the similar beneficial effect of swapping these charges (-/+), whereby the two signaling-deficient single-mutations (-/0) and (+/+) were "rescued" (Fig. 8). In fact, our data do not stand alone. For example, reciprocal mutations between AspII:10 (Asp^{87}) and AsnVII:10 (Asn^{318}) re-established high affinity ligand-binding, thereby rescuing the corresponding (deficient) single-mutations in the gonadotropin-releasing hormone receptor (Zhou et al., 1994). Another example is the angiotensin receptor type 1 where it was shown that the orientation of TM-2 changed in constitutively active mutations compared to wt (Miura and Karnik, 2002). Furthermore, the TLP motif (position II:16-18), conserved among most chemokine receptors, has been shown to be important for receptor activation, as mutation of ThrII:16 to Ala or Val impaired agonist-induced activation in CCR5 (Govaerts et al., 2001a). Interestingly, introduction of Lys or Arg, but not Ala in II:16 rendered CCR2 and -5 constitutive active (Arias et al., 2003). As position II:16 is located one helical turn below II:20, our data correlates very well with these observations. It is possible that the impact of the positive charges in II:16 or II:20 could be ascribed to interactions with negatively charged lipids in the lipid-bilayer.

The interaction between ArgII:20 and IleIII:03 in EBI2 is not of a strong nature (no hydrogen-bond interaction or salt-bridge formation between Arg and Ile), as supported by the unchanged constitutive activity for I(III:03)A (Fig. 6D and Table 2). Interestingly, the importance of TM-II/TM-III interactions has been observed also in other receptors. Thus in CCR5, an interaction of hydrophobic character was shown between PheII:19 and LeuIII:04, since residue swapping rescued a deficient signaling of both single-mutations. Importantly, molecular dynamic simulations indicated that II:20 (Trp in CCR5) created stabilizing aromatic interactions with PheII:19, while a Leu in III:03 stabilized LeuIII:04 in TM-3 (Govaerts et al., 2003). Thus, in a broader perspective, it is possible that the upper segment of TM-2 is involved in the stabilization of active receptor conformations, yet as no consensus sequence is found in this part of TM-2 or

Molecular Pharmacology Fast Forward. Published on July 15, 2008 as DOI: 10.1124/mol.108.049676
This article has not been copyedited and formatted. The final version may differ from this version.

in the surrounding helices (Mirzadegan et al., 2003), this implies that the responsible interaction(s) differ in chemical nature among 7TM receptors. Observations in the NK1 receptor clearly support this notion, as is was shown that Ala substitutions of a series of residues in TM-2 (GluII:10, AsnII:17, AsnII:21, TyrII:24 and AsnII:26) all resulted in an equilibrium-shift between agonist- and antagonist-binding conformations (as measured by B_{max} for radiolabeled agonist and antagonist, respectively) – with a ratio of 1.1 (B_{max}antagonist/B_{max} agonist) for wt NK1 to 4.0-18.5 for the TM-2 mutations (Rosenkilde et al., 1994).

Thus, in summary the activity of EBI2 is regulated by at least two regions with PheVI:13 and surrounding residues acting as negative regulators, and ArgII:20 acting as a positive regulator[4]. In both regions it is most likely that the observed impact is due to conformational changes in the receptor and not a direct interaction with G-proteins in these regions. Importantly, similar impacts have been identified in other 7TM receptors for both regions. It is intriguing, that the impact of TM-2 is rather similar to CCR2 and CCR5 (see above), and that the impact of PheVI:13 is similar to CCR8 and CXCR3 (see above) as EBI2 has been suggested to belong to the chemokine receptors. However, EBI2 does not contain the Glu in the top of TM-7 (VII:06), or the Glu/Asp and Tyr residues often present in the N-termini of chemokine receptors, whereas it does contain part of the conserved TLP in TM-II (ALP in EBI2) and HCC-motif in TM-7 (NCC in EBI2). As a final comment, the constitutive active nature of EBI2 implies that it does not "need" any ligand(s) as it's activity can be controlled simply by adjusting receptor expression from the promoter region, although the observed increase in constitutive activity suggests that there is still "room" for agonism. Given the cellular expression pattern and the upregulation by EBV, it is tempting to ascribe EBI2 a future important role as a target for either antiviral or immune therapy. The present uncovering of the molecular mechanisms for EBI2 activation is important from a drug-development point-of-view, as it may facilitate the rational design and development of small molecule inverse agonists against EBI2.

Molecular Pharmacology Fast Forward. Published on July 15, 2008 as DOI: 10.1124/mol.108.049676
This article has not been copyedited and formatted. The final version may differ from this version.

Acknowledgements

The authors wish to thank Thue W. Schwartz for fruitful discussions and Laura Storjohann for critical reading. The authors would like to thank Inger Smith Simonsen and Lisbet Elbak for excellent technical assistance, Ulrik Gether for the use of the confocal microscope, and Peter Baade, 7TM-pharma for assistance with the receptor alignment.

.

Molecular Pharmacology Fast Forward. Published on July 15, 2008 as DOI: 10.1124/mol.108.049676
This article has not been copyedited and formatted. The final version may differ from this version.

References

Arias DA, Navenot J M, Zhang W B, Broach J and Peiper S C (2003) Constitutive Activation of CCR5 and CCR2 Induced by Conformational Changes in the Conserved TXP Motif in Transmembrane Helix 2. *J Biol Chem* **278**:36513-36521.

Bais C, Santomasso B, Coso O, Arvanitakis L, Raaka E G, Gutkind J S, Asch A S, Cesarman E, Gershengorn M C, Mesri E A and Gerhengorn M C (1998) G-Protein-Coupled Receptor of Kaposi's Sarcoma-Associated Herpesvirus Is a Viral Oncogene and Angiogenesis Activator. *Nature* **391**:86-89.

Baldwin JM (1993) The Probable Arrangement of the Helicee in G Protein-Coupled Receptors. *EMBO J* **12**:1693-1703.

Ballesteros JA and Weinstein H (1995) Integrated methods for the construction of three-dimensional models and computational probing of structure-function relations in G protein-coupled receptors, in *Receptor Molecular Biology* (Sealfon SC ed) pp 366-428, Academic Press, New York.

Beisser PS, Verzijl D, Gruijthuijsen Y K, Beuken E, Smit M J, Leurs R, Bruggeman C A and Vink C (2005) The Epstein-Barr Virus BILF1 Gene Encodes a G Protein-Coupled Receptor That Inhibits Phosphorylation of RNA-Dependent Protein Kinase. *J Virol* **79**:441-449.

Birkenbach M, Josefsen K, Yalamanchili R, Lenoir G and Kieff E (1993) Epstein-Barr Virus-Induced Genes: First Lymphocyte-Specific G Protein-Coupled Peptide Receptors. *J Virol* **67**:2209-2220.

Cherezov V, Rosenbaum D M, Hanson M A, Rasmussen S G, Thian F S, Kobilka T S, Choi H J, Kuhn P, Weis W I, Kobilka B K and Stevens R C (2007) High-Resolution Crystal Structure of an Engineered Human Beta2-Adrenergic G Protein-Coupled Receptor. *Science* **318**:1258-1265.

Elling CE, Frimurer T M, Gerlach L O, Jorgensen R, Holst B and Schwartz T W (2006) Metal-Ion Site Engineering Indicating a Global Toggle Switch Model for 7TM Receptor Activation. *J Biol Chem*.

Farrens DL, Altenbach C, Yang K, Hubbell W L and Khorana H G (1996) Requirement of Rigid-Body Motion of Transmembrane Helices for Light Activation of Rhodopsin. *Science* **274**:768-770.

Govaerts C, Blanpain C, Deupi X, Ballet S, Ballesteros J A, Wodak S J, Vassart G, Pardo L and Parmentier M (2001a) The TXP Motif in the Second Transmembrane Helix of CCR5. A Structural Determinant of Chemokine-Induced Activation. *J Biol Chem* **276**:13217-13225.

Govaerts C, Bondue A, Springael J Y, Olivella M, Deupi X, Le P E, Wodak S J, Parmentier M, Pardo L and Blanpain C (2003) Activation of CCR5 by Chemokines Involves an Aromatic Cluster Between Transmembrane Helices 2 and 3. *J Biol Chem* **278**:1892-1903.

Govaerts C, Lefort A, Costagliola S, Wodak S J, Ballesteros J A, Van S J, Pardo L and Vassart G (2001b) A Conserved Asn in Transmembrane Helix 7 Is an on/Off Switch in the Activation of the Thyrotropin Receptor. *J Biol Chem* **276**:22991-22999.

Holst B, Holliday N D, Bach A, Elling C E, Cox H M and Schwartz T W (2004) Common Structural Basis for Constitutive Activity of the Ghrelin Receptor Family. *J Biol Chem* **279**:53806-53817.

Hubbell WL, Altenbach C, Hubbell C M and Khorana H G (2003) Rhodopsin Structure, Dynamics, and Activation: a Perspective From Crystallography, Site-Directed Spin Labeling, Sulfhydryl Reactivity, and Disulfide Cross-Linking. *Adv Protein Chem* **63**:243-290.

Jensen PC, Nygaard R, Thiele S, Elder A, Zhu G, Kolbeck R, Ghosh S, Schwartz T W and Rosenkilde M M (2007) Molecular Interaction of a Potent Nonpeptide Agonist With the Chemokine Receptor CCR8. *Mol Pharmacol* **72**:327-340.

Kim JM, Altenbach C, Kono M, Oprian D D, Hubbell W L and Khorana H G (2004) Structural Origins of Constitutive Activation in Rhodopsin: Role of the K296/E113 Salt Bridge. *Proc Natl Acad Sci U S A* **101**:12508-12513.

Kostenis E (2002) Potentiation of GPCR-Signaling Via Membrane Targeting of G Protein Alpha Subunits. *J Recept Signal Transduct Res* **22**:267-281.

Marie J, Koch C, Pruneau D, Paquet J L, Groblewski T, Larguier R, Lombard C, Deslauriers B, Maigret B and Bonnafous J C (1999) Constitutive Activation of the Human Bradykinin B2 Receptor Induced by Mutations in Transmembrane Helices III and VI. *Mol Pharmacol* **55**:92-101.

McAllister SD, Hurst D P, Barnett-Norris J, Lynch D, Reggio P H and Abood M E (2004) Structural Mimicry in Class A G Protein-Coupled Receptor Rotamer Toggle Switches: the Importance of the F3.36(201)/W6.48(357) Interaction in Cannabinoid CB1 Receptor Activation. *J Biol Chem* **279**:48024-48037.

Mirzadegan T, Benko G, Filipek S and Palczewski K (2003) Sequence Analyses of G-Protein-Coupled Receptors: Similarities to Rhodopsin. *Biochemistry* **42**:2759-2767.

Miura S and Karnik S S (2002) Constitutive Activation of Angiotensin II Type 1 Receptor Alters the Orientation of Transmembrane Helix-2. *J Biol Chem* **277**:24299-24305.

Muhlemann A, Ward N A, Kratochwil N, Diener C, Fischer C, Stucki A, Jaeschke G, Malherbe P and Porter R H (2006) Determination of Key Amino Acids Implicated in the Actions of Allosteric Modulation by 3,3'-Difluorobenzaldazine on Rat MGlu5 Receptors. *Eur J Pharmacol* **529**:95-104.

Palczewski K, Kumasaka T, Hori T, Behnke C A, Motoshima H, Fox B A, Le T, I, Teller D C, Okada T, Stenkamp R E, Yamamoto M and Miyano M (2000) Crystal Structure of Rhodopsin: A G Protein-Coupled Receptor. *Science* **289**:739-745.

Parma J, Van-Sande J, Swillens S, Tonacchera M, Dumont J and Vassart G (1995) Somatic Mutations Causing Constitutive Activity of the Thyrotropin Receptor Are the Major Cause of Hyperfunctioning Thyroid Adenomas: Identification of Additional Mutations Activating Both the Cyclic Adenosine 3',5'-Monophosphate and Inositol Phosphate-Ca2+ Cascades. *Mol Endocrinol* **9**:725-733.

Paulsen SJ, Rosenkilde M M, Eugen-Olsen J and Kledal T N (2005) Epstein-Barr Virus-Encoded BILF1 Is a Constitutively Active G Protein-Coupled Receptor. *J Virol* **79**:536-546.

Petrel C, Kessler A, Maslah F, Dauban P, Dodd R H, Rognan D and Ruat M (2003) Modeling and Mutagenesis of the Binding Site of Calhex 231, a Novel Negative Allosteric Modulator of the Extracellular Ca(2+)-Sensing Receptor. *J Biol Chem* **278**:49487-49494.

Rasmussen SG, Choi H J, Rosenbaum D M, Kobilka T S, Thian F S, Edwards P C, Burghammer M, Ratnala V R, Sanishvili R, Fischetti R F, Schertler G F, Weis W I and Kobilka B K (2007) Crystal Structure of the Human Beta2 Adrenergic G-Protein-Coupled Receptor. *Nature* **450**:383-387.

Robbins LS, Nadeau J H, Johnson K R, Kelly M A, Roselli-Rehfuss L, Baack E, Mountjoy K G and Cone R D (1993) Pigmentation Phenotypes of Variant Extension Locus Alleles Result From Point Mutations That Alter MSH Receptor Function. *Cell* **72**:1-20.

Rosenkilde MM, Andersen M B, Nygaard R, Frimurer T M and Schwartz T W (2007) Activation of the CXCR3 Chemokine Receptor Through Anchoring of a Small Molecule Chelator Ligand Between TM-III, -IV, and -VI. *Mol Pharmacol* **71**:930-941.

Rosenkilde MM, Benned-Jensen T, Andersen H, Holst P J, Kledal T N, Luttichau H R, Larsen J K, Christensen J P and Schwartz T W (2006) Molecular Pharmacological Phenotyping of EBI2. An Orphan Seven-Transmembrane Receptor With Constitutive Activity. *J Biol Chem* **281**:13199-13208.

Rosenkilde MM, Cahir M, Gether U, Hjorth S A and Schwartz T W (1994) Mutations Along Transmembrane Segment II of the NK-1 Receptor Affect Substance P Competition With Non-Peptide Antagonists but Not Substance P Binding. *J Biol Chem* **269**:28160-28164.

Rosenkilde MM, Kledal T N, Brauner-Osborne H and Schwartz T W (1999) Agonists and Inverse Agonists for the Herpesvirus 8-Encoded Constitutively Active Seven-Transmembrane Oncogene Product, ORF-74. *J Biol Chem* **274**:956-961.

Roth BL, Shoham M, Choudhary M S and Khan N (1997) Identification of Conserved Aromatic Residues Essential for Agonist Binding and Second Messenger Production at 5-Hydroxytryptamine2A Receptors. *Mol Pharmacol* **52**:259-266.

Schwartz TW (1994) Locating Ligand-Binding Sites in 7TM Receptors by Protein Engineering. *Curr Opin Biotech* **5**:434-444.

Schwartz TW, Frimurer T M, Holst B, Rosenkilde M M and Elling C E (2006) Molecular Mechanism of 7tm Receptor Activation-a Global Toggle Switch Model. *Annu Rev Pharmacol Toxicol* **46**:481-519.

Seifert R and Wenzel-Seifert K (2002) Constitutive Activity of G-Protein-Coupled Receptors: Cause of Disease and Common Property of Wild-Type Receptors. *Naunyn Schmiedebergs Arch Pharmacol* **366**:381-416.

Shi L, Liapakis G, Xu R, Guarnieri F, Ballesteros J A and Javitch J A (2002) Beta2 Adrenergic Receptor Activation. Modulation of the Proline Kink in Transmembrane 6 by a Rotamer Toggle Switch. *J Biol Chem* **277**:40989-40996.

Srinivasan S, Santiago P, Lubrano C, Vaisse C and Conklin B R (2007) Engineering the Melanocortin-4 Receptor to Control Constitutive and Ligand-Mediated G(S) Signaling in Vivo. *PLoS ONE* **2**:e668.

Vassilatis DK, Hohmann J G, Zeng H, Li F, Ranchalis J E, Mortrud M T, Brown A, Rodriguez S S, Weller J R, Wright A C, Bergmann J E and Gaitanaris G A (2003) The G Protein-Coupled Receptor Repertoires of Human and Mouse. *Proc Natl Acad Sci U S A* **100**:4903-4908.

Zhou W, Flanagan C, Ballesteros J A, Konvicka K, Davidson J S, Weinstein H, Millar R P and Sealfon S C (1994) A Reciprocal Mutation Supports Helix 2 and Helix 7 Proximity in the Gonadotropin-Releasing Hormone Receptor. *Mol Pharmacol* **45**:165-170.

Molecular Pharmacology Fast Forward. Published on July 15, 2008 as DOI: 10.1124/mol.108.049676
This article has not been copyedited and formatted. The final version may differ from this version.

Footnotes

a) *Un-numbered footnote to the Title: The study was supported from the Danish Medical Research Council, the NovoNordisk Foundation, the Carlsberg Foundation, and the Aase and Ejnar Danielsen Foundation, the AP-Moller foundation and the European Community's Sixth Framework Program (INNOCHEM : LSHB-CT-2005-518167).

b) Reprint request to: Mette M. Rosenkilde, Laboratory for Molecular Pharmacology,
Department of Neuroscience and Pharmacology, The Panum Institute,
Copenhagen University, Blegdamsvej 2, 2200 Copenhagen, Denmark,
Phone: 0045 61364871, Fax: 0045 35327610, e-mail: rosenkilde@sund.ku.dk

c) Numbered footnotes:

[1] In the text we use the generic 7TM numbering system suggested by Baldwin (Baldwin, 1993), and later modified by Schwartz (Schwartz, 1994), whereas we in the tables in addition include the nomenclature suggested by Ballesteros & Weinstein (Ballesteros and Weinstein, 1995).

[2] Due to the orphan status of EBI2, the term “major binding pocket” is used in a broader perspective, as robust experimental evidence support that the helices in rhodopsin-like 7TM receptors form a major and a minor binding pocket (delimited by TM-3 to -7 in the case of the major and TM-1 to -3 and TM-7 for the minor binding pocket).

[3] (x,y) designates the charges at II:20 (x) and III:03 (y), in which “+” is positive, “-“ is negative and “0” is neutral.

[4] The modulation of constitutive activity by mutagenesis, and the many different cell-and membrane-based assays for which constitutive activity have been shown, see (Rosenkilde et al., 2006) and the GTPγS-binding in Fig. 2 (present paper), supports the ligand-independent “constitutive” nature, i.e. that the activity in not caused by an unknown agonist in the medium.

Molecular Pharmacology Fast Forward. Published on July 15, 2008 as DOI: 10.1124/mol.108.049676
This article has not been copyedited and formatted. The final version may differ from this version.

Legends for figures

Fig. 1. Serpentine (A) and helical wheel (B) models of the human EBI2 receptor. Grey circles indicate mutated residues substituted to either reduce or increase the size of the side chain or to change the charge. Black background with white letter indicates the most conserved residues in each helix. In addition the positions of the conserved amino acids are indicated next to the black circles.

Fig. 2. EBI2 is a constitutively active 7TM receptor. (A) HEK293 cells were transiently transfected with Gqi4myr, reporter plasmid (CREB/Luc system) and increasing concentrations of FLAG-tagged EBI2 receptor or pcDNA (0, 5, 15, and 25 ng/80,000 cells). A representative example is shown. (B) HEK293 cells were transiently transfected with reporter plasmid (CREB/Luc system) and increasing concentrations of FLAG-tagged EBI2 receptor or pcDNA (0, 5, 15, and 25 ng/80,000 cells). On the assay day, the cAMP production was induced by incubating the cells in growth medium containing 15 μM forskolin. A representative example is shown. (C) [^{35}S]GTPγS binding to membranes isolated from naïve HEK293 cells and HEK293 cells stably expressing FLAG-tagged EBI2 receptor (left) or induced (+Dox; doxycline at 5 ng/mL) or uninduced (-Dox) TREX-HEK293 cells stably transfected with FLAG-tagged EBI2 receptor (right). The data are mean ± S.E.M of three independent experiments performed in triplicates. *, $p < 0.05$ and **, $p < 0.01$. (D) [^{35}S]GTPγS binding to membranes isolated from naïve L1.2 pre-B-cells and L1.2 cells stably expressing C-terminally GFP-tagged EBI2 receptor. The data are mean ± S.E.M of three independent experiments performed in triplicates. ***, $p < 0.001$.

Fig. 3. PheVI:13 in the conserved CFxP-motif is important for the regulation of constitutive activity. HEK293 cells were transiently transfected with Gqi4myr, the reporter plasmid (CREB/Luc system) and increasing concentrations of FLAG-tagged EBI2 receptor (0, 5, 15, and 25 ng/80,000 cells). (A) The relative constitutive activity of the Ala, Cys, and Trp-introductions in VI:13: F(VI:13A)-, F(VI:13)C-, and F(VI:13)W-EBI2 were calculated from the observed CREB-activation (B), correlated to cell-surface expression (C). The CREB-activation was determined for 0, 5, 15, and 25 ng receptor/80.000 cells (B), while the cell surface expression was determined at 15 as well as 25 ng receptor/80.000 cells. The relative

Molecular Pharmacology Fast Forward. Published on July 15, 2008 as DOI: 10.1124/mol.108.049676
This article has not been copyedited and formatted. The final version may differ from this version.

constitutive activity was determined for both concentrations (see Table 1), and the values for 15ng/80.000 cells are depicted in A. All experiments (in B and C) were performed in parallel, and wt EBI2 was included in all experiments (N>3). (D-F) Confocal microscopy of EBI2 wt (D), F(VI:13)A- (E), and F(VI:13)C-EBI2 (F). Briefly, HEK293 cells were transiently transfected with 150 ng receptor /80.000 cells, fixed 48 hours after transfection and the cell surface EBI2 expression visualized by the anti-FLAG M1 antibody followed by the Alexa Fluor 488-conjugated IgG antibody. The confocal microscopy was performed using a LSM 510 laser scanning unit coupled to an inverted microscope with an oil immersion Plan-Apochromat objective (Carl Zeiss).

Fig. 4. Correlation of receptor activation and surface expression for multiple DNA concentrations. (A) HEK293 cells were transiently transfected with Gqi4myr, the reporter plasmid (CREB/Luc system) and 12 concentrations of FLAG-tagged wt EBI2 receptor (0-35 ng/80.000 cells), and the activity was determined in parallel with surface expression for all DNA concentrations. A linear regression of the data is indicated by the line. Supplemental Fig. 1 shows the corresponding individual experiments. (B) Data extracted from similar gene-dose experiments with the Ala and Cys-introduction in VI:13, where the white columns indicate receptor expression, and the black columns indicate receptor activity. Supplemental Fig. 2 shows the correlation for all included DNA concentrations. (N>3).

Fig. 5. The role of TM-6 and residues nearby for 7TM receptor activation. The experiments were performed as described in Fig. 3. (A-C) Relative constitutive activity (A), observed CREB-activation (B), and surface expression (C) for the mutations in the two other aromatic residues in TM-6 (PheVI:09 and TyrVI:16). (D-F) Relative constitutive activity (D), observed CREB-activation (E), and surface expression (F) for the mutations in TM-7 (ValVI:06 and MetVII:09). (N>3). Molecular model showing PheVI:13 and the surrounding residues in EBI2 based on the crystal structure of rhodopsin and rendered wih PyMOL software. TM-6 (blue) and TM-7 (grey) are seen from the major binding pocket, with the positions of ProVI:15 and ProVII:17 marked in red.

Molecular Pharmacology Fast Forward. Published on July 15, 2008 as DOI: 10.1124/mol.108.049676
This article has not been copyedited and formatted. The final version may differ from this version.

Fig. 6. ArgII:20 is important for EBI2 activity, and interaction with III:03 stabilizes the activity. The experiments were performed as described in Fig. 3. (A-C) Relative constitutive activity (A), observed CREB-activation (B), and surface expression (C) for the Ala, Glu, and Lys introduction in II:20 in substitution of Arg. (D-F) Relative constitutive activity (D), observed CREB-activation (E), and surface expression (F) for the Ala, Glu, and Arg introduction in III:03 in substitution of Ile. (N>3).

Fig. 7. Charge swap between II:20 and III:03 rescues activity of EBI2. The experiments were performed as described in Fig. 3. (A-C) Relative constitutive activity (A), observed CREB-activation (B), and surface expression (C) for the two double mutations: swap of charges ((+/-), shown in Fig. 6D) to (-/+)) by Glu introduction in II:20 and Arg introduction in III:03Ala (white column), and introduction of Glu at both positions (-/-) (grey column) (N>3). (D-G) Confocal microscopy of the single and double mutations involving Glu and Arg introduction in III:03, either as single mutations (D and E, respectively) or combined with substitution of ArgII:20 to Glu (F and G, respectively). The confocal microscopy was performed as described in Fig. 3.

Fig. 8 Summary of the beneficial impact of the electrostatic interaction between position II:20 and III:03. (A) Helical wheel model emphasizing the positions of interest: II:20 and III:03. (B) Rescue of the two signaling-deficient single-mutations: Glu introduction in II:20 (-/0) and Arg introduction in III:03 (+/+), embedded from Fig. 6A and 5D, respectively by combining these two mutations (-/+), embedded from Fig. 7A) to signaling levels similar to the (+/-) salt-bridge formation from Glu introduction in III:03, embedded from Fig. 3A. (C) Molecular model showing the proximity of ArgII:20 and IleIII:03 based on the crystal structure of rhodopsin and rendered wih PyMOL software. TM-2 (blue) and TM-3 (grey) as seen from the minor binding pocket, with the positions of ProII:18 marked in red.

Fig. 9 Inhibition of forskolin-induced cAMP production by EBI2 wt and selected mutants. HEK293 cells were transiently transfected with reporter vector (CREB/Luc system) and increasing concentrations of FLAG-tagged EBI2 wt or mutant contructs (0, 5, 15 and 25 ng/80,000 cells for A-D and 0,15 and 25

ng/80,000 cells for E-F). To stimulate cAMP production, the cells were incubated with forskolin (fsk, 15 μM) and, when present, pertussis toxin (ptx, 100 ng/mL). (A-D) Inhibition of forskolin-induced CREB activity by (A) EBI2 wt and pcDNA in the presence or absence of pertussis toxin, (B) the II:20 mutants (R(II:20)A/E/K), (C) selected III:03 mutants (I(III:03)E/R) and (D) the double "charge-swap" mutants (R(II:20)E-I(III:03)E (-/-) and R(II:20)E-I(III:03)R (-/+)). The stabled and dotted lines in (B-D) indicate EBI2 wt and pcDNA (taken from (A)), respectively. Results are given relative to forskolin-stimulated cells transfected with reporter vector only (0 ng/80,000 cells) in percent ± SEM (N = 2-5). (E-F) Cell surface expression of EBI2 wt and mutants measured by ELISA. Results are given relative to EBI2 wt at 15ng/80,000 cells in percent ± SEM (N = 2-5).

Molecular Pharmacology Fast Forward. Published on July 15, 2008 as DOI: 10.1124/mol.108.049676
This article has not been copyedited and formatted. The final version may differ from this version.

TABLE 1. Mutations in the EBI2 major binding pocket. EBI2 mutations were assessed for their cell surface expression and ability to activate the CREB transcription factor in transiently transfected HEK293 cells. The table shows these values at 15 ng/80.000 cells and the relative constitutive activity (see *Materials and Methods* for calculation) at 15 and 25 ng/80.000 cells. The latter is highlighted as follows: mutations with values (at both gene doses) between 2.00 and 4.00: light green and above 4.00: dark green. CREB activity and cell surface expression are presented as percent ± SEM, whereas the relative constitutive activity is presented as fold ± SEM. In all cases, the results are given relative to the wt value. The number of experiments is given as *n*. Receptor residues are presented according to the Schwartz and Ballesteros/Weinstein (Ballest.) nomenclatures (see footnote 1 in the text). Furthermore, the three most common amino acids at the particular position are given.

	Residue					CREB act. (15 ng/well,%)		Expression (15 ng/well,%)		Relative CA (15 ng,fold)		Relative CA (25 ng,fold)		(n)
	Mutation	*Number*	*Schwartz*	*Ballest*	*3 most common aa*	*Mean*	*SEM*	*Mean*	*SEM*	*Mean*	*SEM*	*Mean*	*SEM*	
TM III	T(III:04)A	T107	Thr III:04	T3.28	V:19%,S:10%,W:10%	97	3.2	94	1.6	1.0	0.05	1.1	0.07	(3)
	T(III:04)E	–				76	12	53	11	1.4	0.08	1.2	0.06	(4)
	F(III:08)A	F111	Phe III:08	F3.32	D:20%,F:15%,L:9%	78	10	108	18	0.74	0.05	0.82	0.04	(6)
	F(III:08)Y	–				73	11	39	6.4	1.9	0.11	1.8	0.14	(6)
	T(III:12)A	T115	Thr III:12	T3.36	M:20%,L:15%,V:11%	116	10	126	31	0.93	0.07	1.2	0.09	(3)
	T(III:12)F	–				142	41	310	91	0.46	0.01	0.68	0.09	(4)
TM V	C(V:09)A	C201	Cys V:09	C5.43	F:23%,L:13%,S:10%	45	5.9	71	7.5	0.63	0.07	0.68	0.07	(4)
	G(V:12)W	G204	Gly V:12	C5.46	G:29%,L:14%,A:11%	40	2.7	66	5.2	0.61	0.03	0.64	0.04	(4)
	Y(V:13)A	Y205	Tyr V:13	C5.47	F:70%,Y:11%,L:4%	38	4.7	54	9.2	0.70	0.08	0.64	0.03	(4)
	Y(V:13)F	–				86	7.3	61	14	1.4	0.13	1.4	0.10	(4)
TM VI	F(VI:09)A	F253	Phe VI:09	F6.44	F:82%,Y:6%,L:3%	75	1.4	81	8.9	0.91	0.10	1.0	0.07	(5)
	C(VI:12)A	C256	Cys VI:12	C6.47	C:74%,S:9%,F:5%	95	1.8	41	1.6	**2.3**	**0.21**	**2.4**	**0.19**	(4)
	F(VI:13)A	F257	Phe VI:13	F6.48	W:71%,F:16%,Q:2%	39	7.5	7.0	1.1	**5.7**	**0.50**	**4.7**	**0.27**	(5)
	F(VI:13)C	–				54	8.3	17	1.8	**3.1**	**0.27**	**4.8**	**0.27**	(6)
	F(VI:13)W	–				67	5.3	73	11	0.9	0.08	1.0	0.13	(4)
	Y(VI:16)A	Y260	Tyr VI:16	Y6.51	Y:36%,F:30%,L:12%	25	3.6	57	7.3	0.43	0.04	0.53	0.07	(6)
	Y(VI:16)F	–				49	4.7	96	15	0.53	0.03	0.59	0.14	(5)
	M(VI:24)A	M268	Met VI:24	M6.59	A:16%,T:14%,L:12%	89	4.7	109	9.2	0.82	0.07	0.84	0.07	(5)
TM VII	T(VII:05)A	T293	Thr VII:05	T7.38	T:24%,A:15%,S:13%	99	7.1	126	8.0	0.87	0.05	0.69	0.13	(6)
	V(VII:06)A	V294	Val VII:06	V7.39	L:21%,V:11%,T:11%	110	11	88	5.9	1.3	0.07	1.4	0.10	(4)
	M(VII:09)A	M297	Met VII:09	M7.42	A:40%,G:20%,S:13%	65	2.3	93	2.2	0.71	0.02	0.78	0.05	(4)
	M(VII:09)F	–				85	15	80	2.9	1.1	0.06	1.4	0.15	(4)
	N(VII:12)A	N300	Asn VII:12	N7.45	N:67%,S:12%,H:9%	103	5.8	146	20	0.73	0.08	0.81	0.11	(3)

Molecular Pharmacology Fast Forward. Published on July 15, 2008 as DOI: 10.1124/mol.108.049676
This article has not been copyedited and formatted. The final version may differ from this version.

TABLE 2. Mutations in the EBI2 minor binding pocket and extracellular loop 2. EBI2 mutations were assessed for their cell surface expression and ability to activate the CREB transcription factor in transiently transfected HEK293 cells. The table shows these values at 15 ng/80.000 cells and the relative constitutive activity (see *Materials and Methods* for calculation) at 15 and 25 ng/80.000 cells. The latter is highlighted as follows: mutations with values (at both gene doses) between 0 and 0.25: red, 0.25 – 0.50: orange, 2.00 – 4.00: light green and above 4.00: dark green. CREB activity and cell surface expression are presented as percent ± SEM, whereas the relative constitutive activity is presented as fold ± SEM. In all cases, the results are given relative to the wt value. The number of experiments is given as *n*. Receptor residues are presented according to the Schwartz and Ballesteros/Weinstein (Ballest.) nomenclatures (see footnote 1 in the text). Furthermore, the three most common amino acids at the particular position are given.

	Residue					CREB act. (15 ng/well,%)		Expression (15 ng/well,%)		Relative CA (15 ng,fold)		Relative CA (25 ng,fold)		(n)
	Mutation	*Number*	*Schwartz*	*Ballest*	*3 most common aa*	*Mean*	*SEM*	*Mean*	*SEM*	*Mean*	*SEM*	*Mean*	*SEM*	
TM II	F(II:13)A	F80	Phe II:13	F2.53	V:24%,F:19%,L:17%	97	8.8	108	7.7	0.90	0.05	0.86	0.02	(6)
	L(II:17)A	L84	Leu II:17	L2.57	L:39%,V:14%,C:12%	93	7.3	103	8.8	0.90	0.04	0.81	0.03	(4)
	R(II:20)A	R87	Arg II:20	R2.60	L:20%,F:16%,W:15%	9.1	1.4	70	13	**0.14**	**0.02**	**0.16**	**0.03**	(5)
	R(II:20)E	–				21	3.6	77	3.0	**0.26**	**0.04**	**0.40**	**0.04**	(4)
	R(II:20)K	–				76	7.9	88	13	0.86	0.06	0.86	0.07	(4)
	Y(II:24)A	Y91	Tyr II:24	Y2.64	Y:21%,V:13%,L:10%	108	19	107	19	1.0	0.07	1.0	0.15	(7)
TM III	I(III:03)A	I106	Ile III:03	I3.27	L:31%,V:21%,P:14%	89	7.5	77	11	1.2	0.06	1.1	0.13	(3)
	I(III:03)E	–				26	3.8	6.0	1.0	**4.4**	**0.09**	**3.8**	**0.19**	(3)
	I(III:03)R	–				4.2	0.6	19	1.6	**0.22**	**0.04**	**0.20**	**0.05**	(6)
	V(III:07)A	V110	Val III:07	V3.31	L:39%,I:15%,V:12%	108	10	94	6.5	1.2	0.07	1.2	0.07	(5)
TM VII	H(VII:03)A	H291	His VII:03	H7.36	L:12%,I:7%,H:7%	52	5.7	51	11	0.97	0.16	0.87	0.07	(3)
	N(VII:10)A	N298	Asn VII:10	N7.43	Y:33%,F:14%,S:13%	95	5.9	111	12	0.86	0.08	0.94	0.08	(4)
	N(VII:10)Y	–				37	9.8	81	4.1	**0.44**	**0.07**	**0.44**	**0.08**	(4)
	C(VII:14)A	C302	Cys VII:14	C7.47	C:42%,A:11%,V:10%	51	4.8	60	10	0.86	0.07	1.1	0.07	(4)
Double	R(II:20)E- I(III:03)R	R087- I106	Arg II:20- Ile III:03	R2.60- I3.27		19	0.6	7.1	0.8	**2.7**	**0.29**	**2.2**	**0.18**	(3)
	R(II:20)E- I(III:03)E	– –				3.6	1.6	6.2	0.9	0.55	0.17	0.69	0.11	(3)
ECL2	E183A					45	3.7	61	7.0	0.76	0.02	0.69	0.05	(7)
	E175A-E177A					89	3.4	80	8.9	1.1	0.09	1.3	0.04	(3)
	E188A-E189A					95	4.2	69	9.3	1.3	0.16	1.3	0.03	(4)
	E175A-E177A-E183A					47	6.0	64	7.9	0.74	0.01	0.58	0.07	(3)
	E183A-E188A-E189A					42	2.6	77	2.6	0.54	0.02	0.51	0.03	(3)

Figure 1

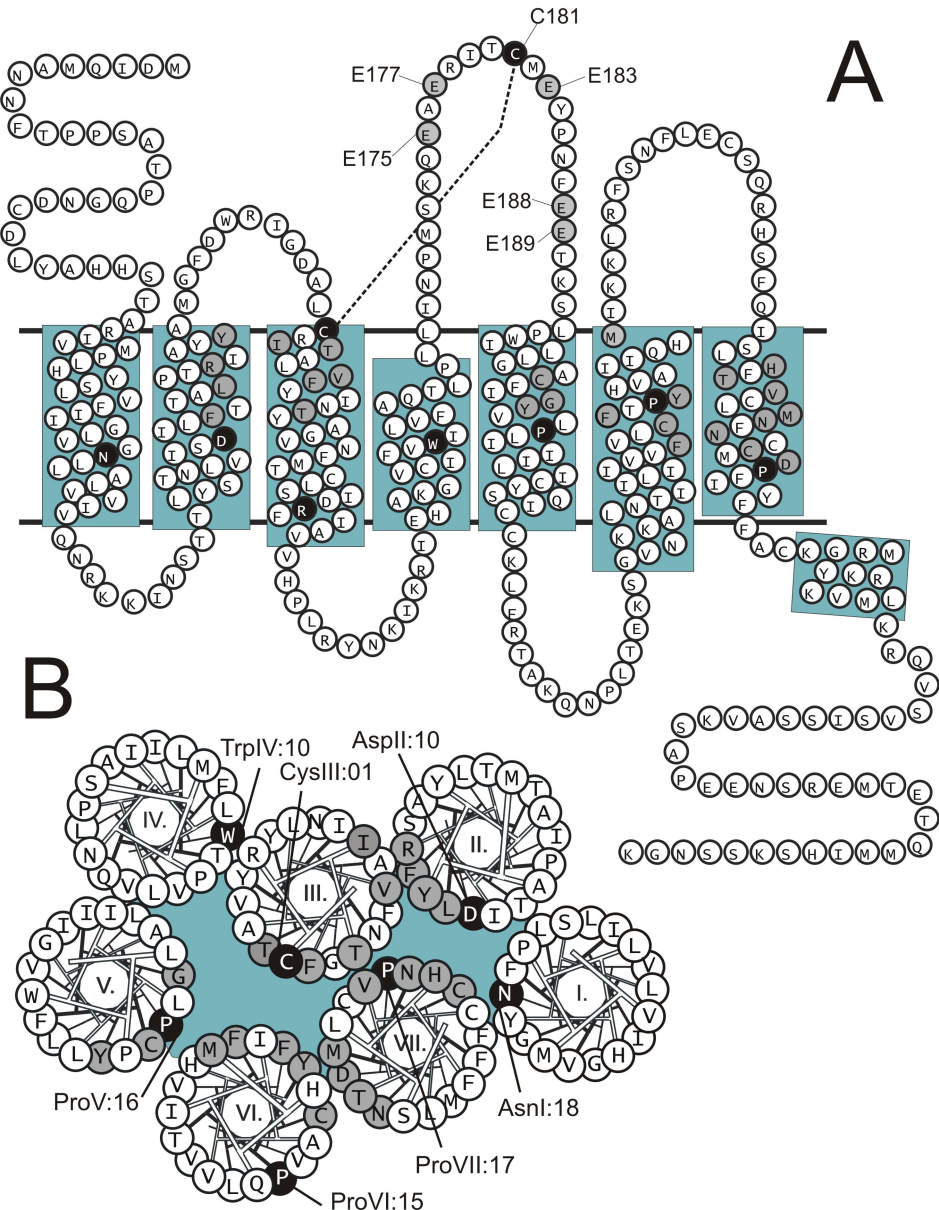
A
C181
E177
E183
E175
E188
E189
B
TrpIV:10
CysIII:01
AspII:10
ProV:16
AsnI:18
ProVII:17
ProVI:15
IV.
II.
III.
V.
I.
VII.
VI.

Figure 2

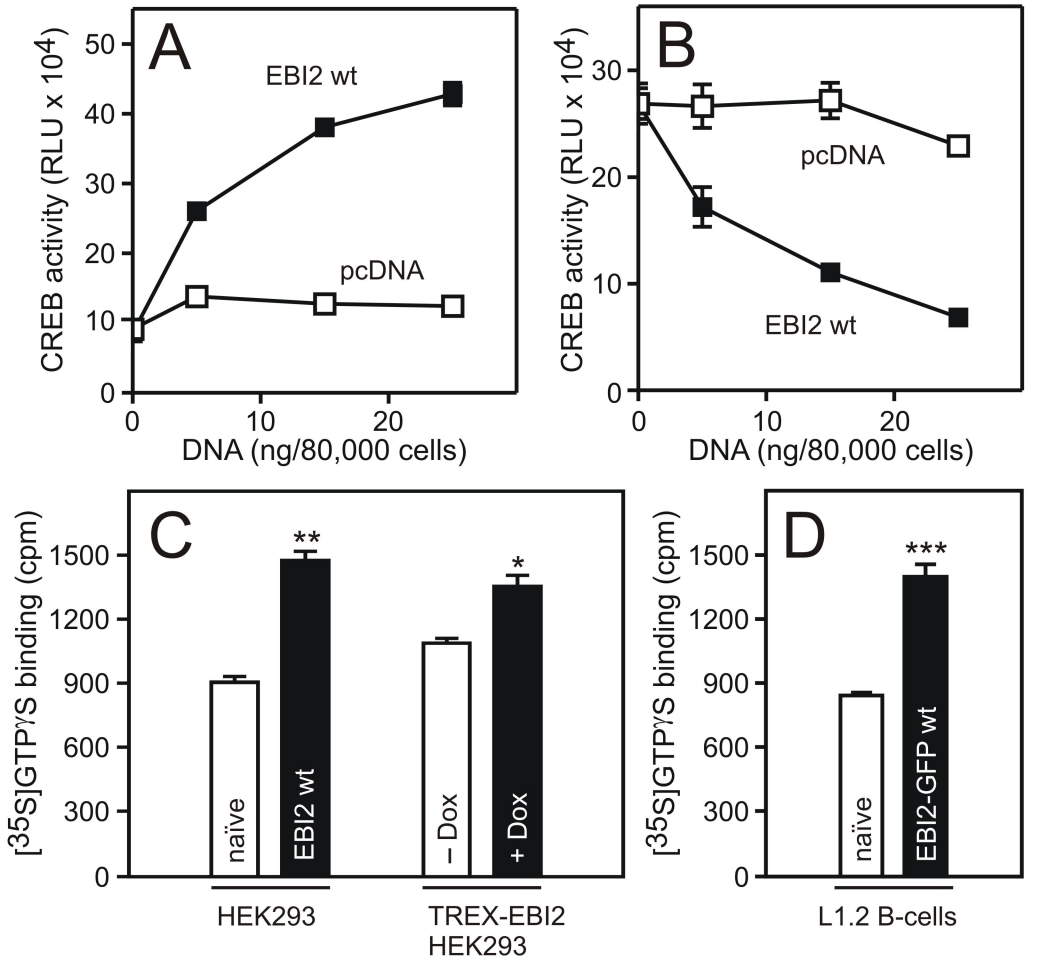
A
EBI2 wt
pcDNA
CREB activity (RLU x 10^4)
DNA (ng/80,000 cells)
B
pcDNA
EBI2 wt
CREB activity (RLU x 10^4)
DNA (ng/80,000 cells)
C
[35S]GTPγS binding (cpm)
naïve
EBI2 wt
– Dox
+ Dox
HEK293
TREX-EBI2 HEK293
D
[35S]GTPγS binding (cpm)
naïve
EBI2-GFP wt
L1.2 B-cells

Figure 3

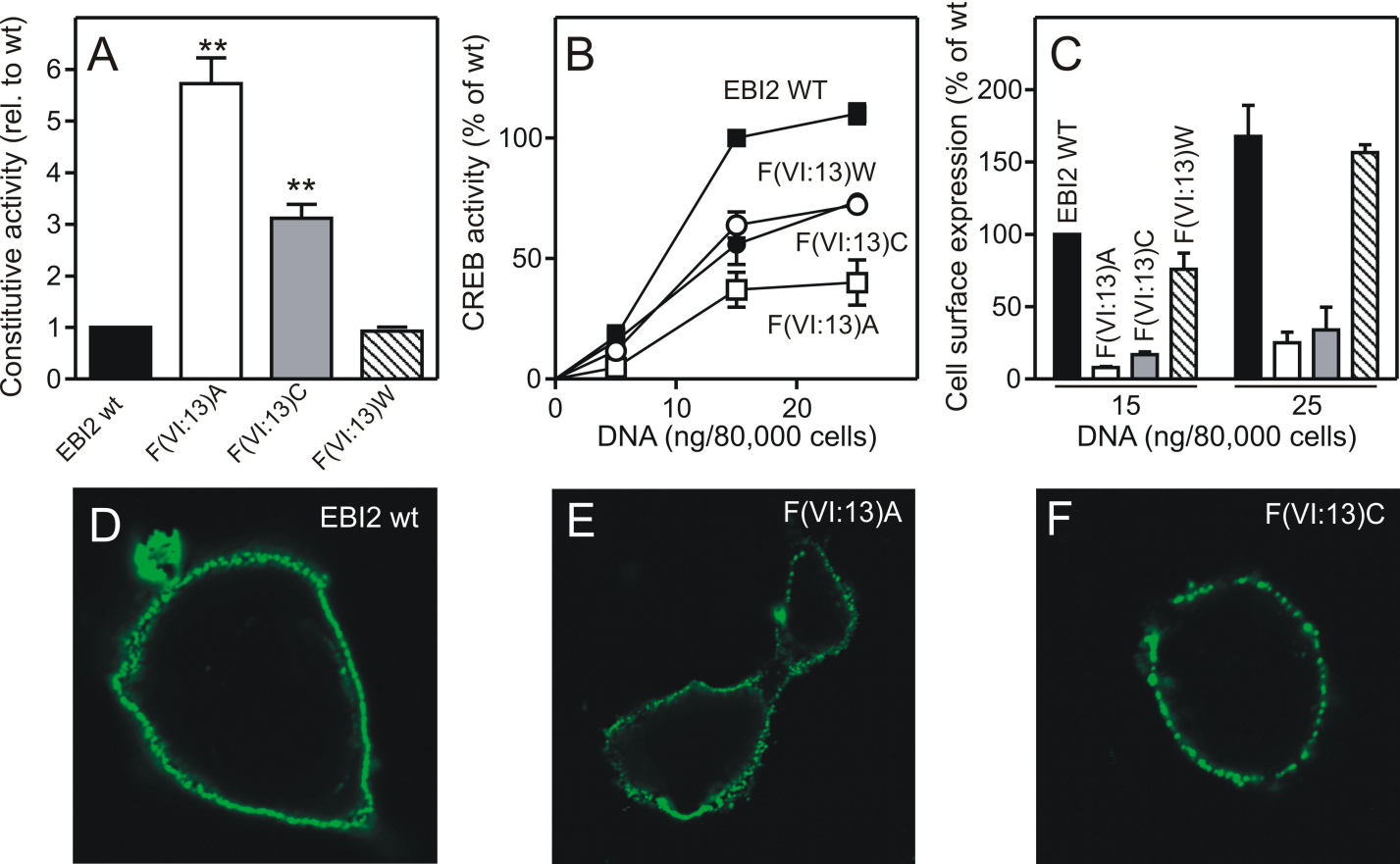
A
Constitutive activity (rel. to wt)
**
**
EBI2 wt
F(VI:13)A
F(VI:13)C
F(VI:13)W
B
CREB activity (% of wt)
EBI2 WT
F(VI:13)W
F(VI:13)C
F(VI:13)A
DNA (ng/80,000 cells)
C
Cell surface expression (% of wt)
EBI2 WT
F(VI:13)A
F(VI:13)C
F(VI:13)W
15
25
DNA (ng/80,000 cells)
D
EBI2 wt
E
F(VI:13)A
F
F(VI:13)C

Figure 4

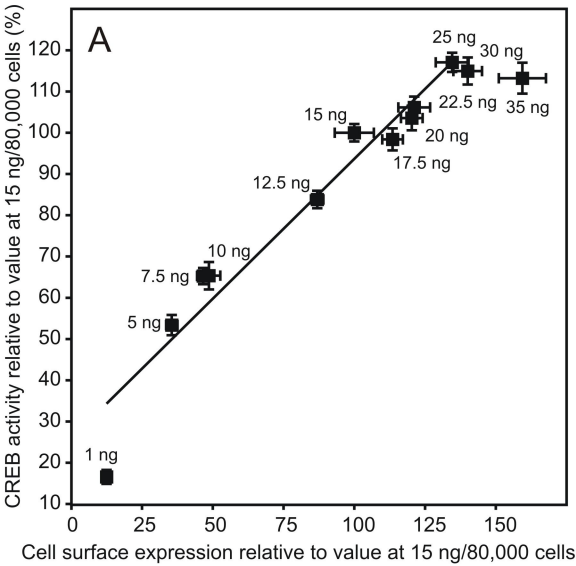
A
CREB activity relative to value at 15 ng/80,000 cells (%)
Cell surface expression relative to value at 15 ng/80,000 cells (%)
1 ng
5 ng
7.5 ng
10 ng
12.5 ng
15 ng
17.5 ng
20 ng
22.5 ng
25 ng
30 ng
35 ng

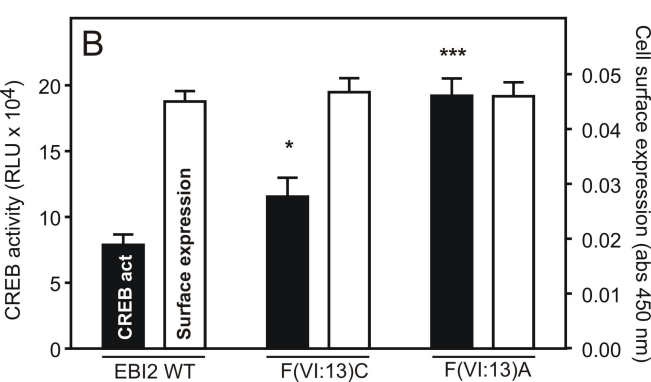
B
CREB activity (RLU x 10^4)
Cell surface expression (abs 450 nm)
CREB act
Surface expression
*
***
EBI2 WT
F(VI:13)C
F(VI:13)A

Figure 5

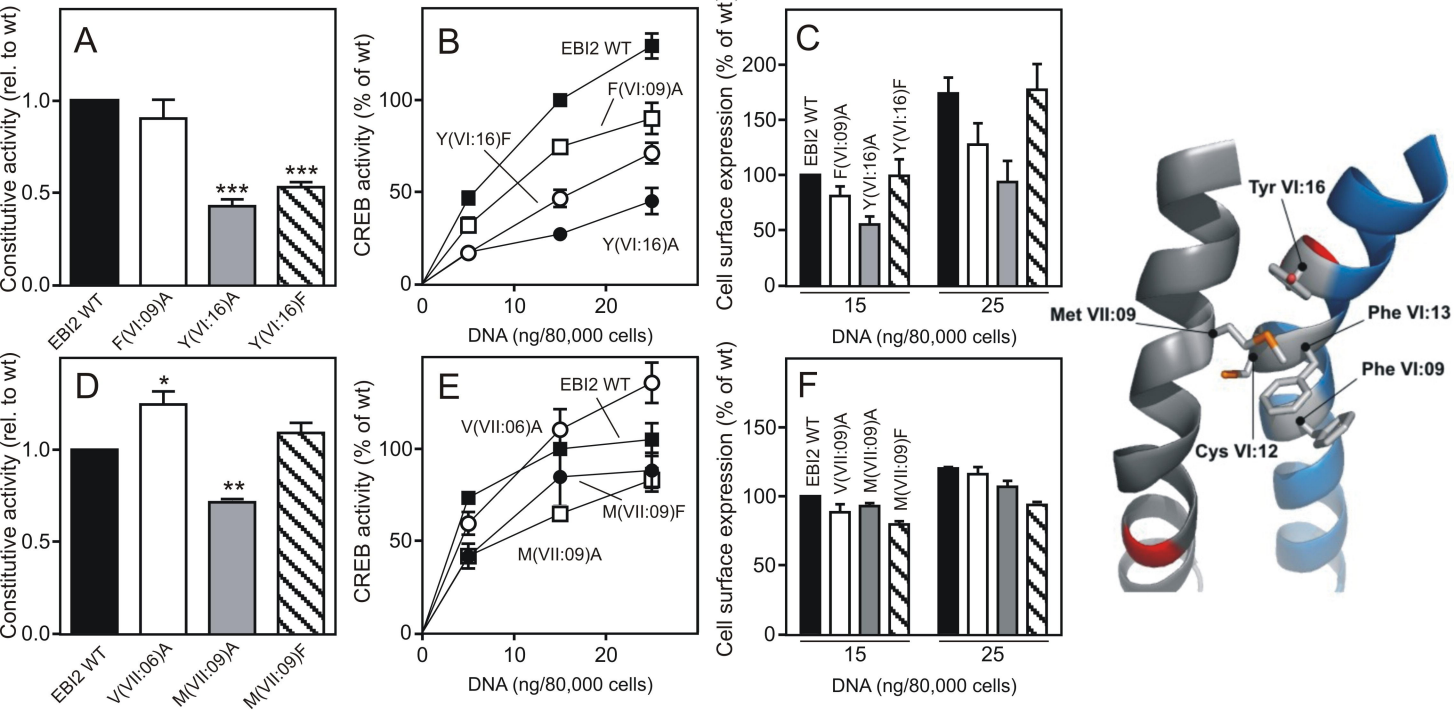
A
Constitutive activity (rel. to wt)
1.0
0.5
0.0
***
***
EBI2 WT
F(VI:09)A
Y(VI:16)A
Y(VI:16)F
B
CREB activity (% of wt)
100
50
0
EBI2 WT
F(VI:09)A
Y(VI:16)F
Y(VI:16)A
0
10
20
DNA (ng/80,000 cells)
C
Cell surface expression (% of wt)
200
150
100
50
0
EBI2 WT
F(VI:09)A
Y(VI:16)A
Y(VI:16)F
15
25
DNA (ng/80,000 cells)
Tyr VI:16
Met VII:09
Phe VI:13
Phe VI:09
Cys VI:12
D
Constitutive activity (rel. to wt)
1.0
0.5
0.0
*
**
EBI2 WT
V(VII:06)A
M(VII:09)A
M(VII:09)F
E
CREB activity (% of wt)
100
50
0
EBI2 WT
V(VII:06)A
M(VII:09)F
M(VII:09)A
0
10
20
DNA (ng/80,000 cells)
F
Cell surface expression (% of wt)
150
100
50
0
EBI2 WT
V(VII:09)A
M(VII:09)A
M(VII:09)F
15
25
DNA (ng/80,000 cells)

Figure 6

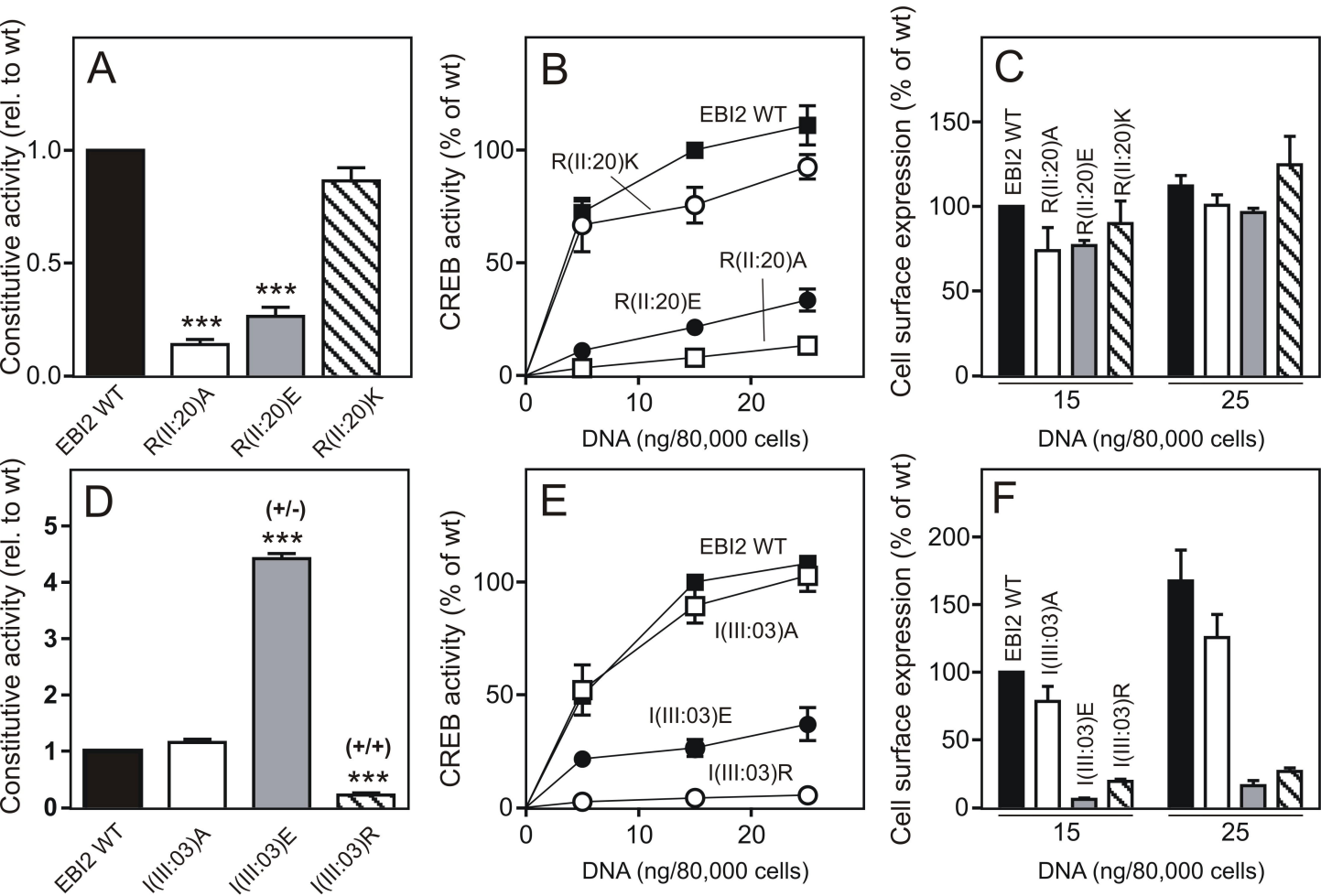
A
Constitutive activity (rel. to wt)
1.0
0.5
0.0
***
***
EBI2 WT
R(II:20)A
R(II:20)E
R(II:20)K
B
CREB activity (% of wt)
EBI2 WT
R(II:20)K
R(II:20)A
R(II:20)E
100
50
0
0
10
20
DNA (ng/80,000 cells)
C
Cell surface expression (% of wt)
EBI2 WT
R(II:20)A
R(II:20)E
R(II:20)K
150
100
50
0
15
25
DNA (ng/80,000 cells)
D
Constitutive activity (rel. to wt)
5
4
3
2
1
0
(+/-)
***
(+/+)
***
EBI2 WT
I(III:03)A
I(III:03)E
I(III:03)R
E
CREB activity (% of wt)
EBI2 WT
I(III:03)A
I(III:03)E
I(III:03)R
100
50
0
0
10
20
DNA (ng/80,000 cells)
F
Cell surface expression (% of wt)
EBI2 WT
I(III:03)A
I(III:03)E
I(III:03)R
200
150
100
50
0
15
25
DNA (ng/80,000 cells)

Figure 7

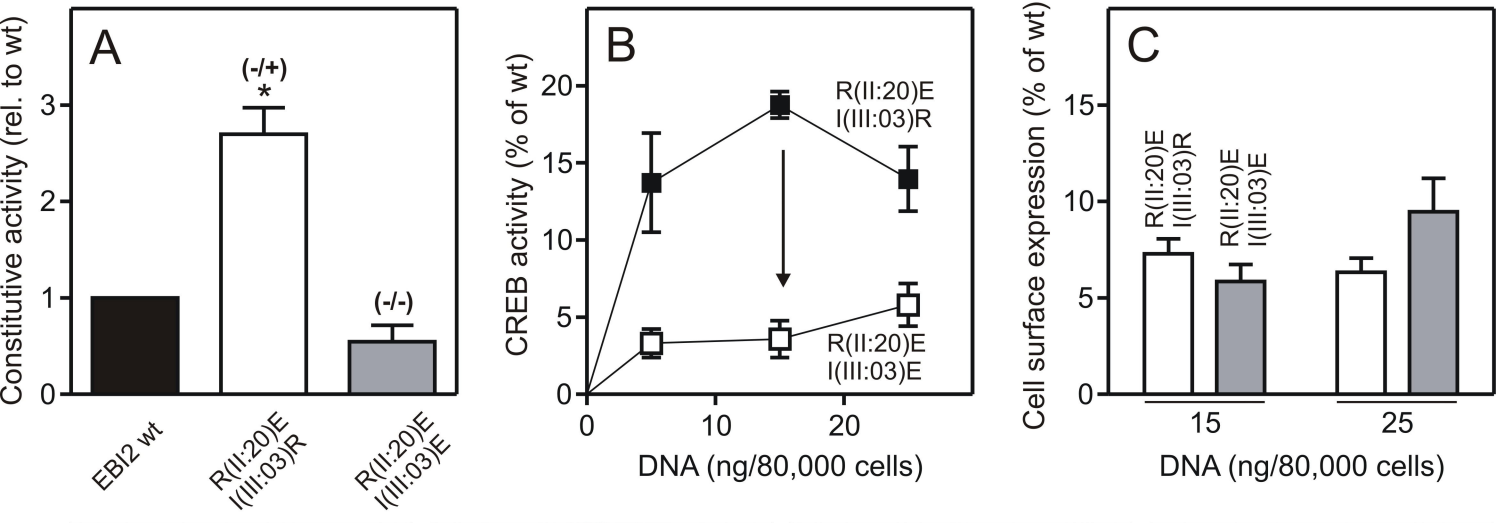
A
Constitutive activity (rel. to wt)
(-/+)
*
(-/-)
EBI2 wt
R(II:20)E
I(III:03)R
R(II:20)E
I(III:03)E
B
CREB activity (% of wt)
R(II:20)E
I(III:03)R
R(II:20)E
I(III:03)E
DNA (ng/80,000 cells)
C
Cell surface expression (% of wt)
R(II:20)E
I(III:03)R
R(II:20)E
I(III:03)E
15
25
DNA (ng/80,000 cells)

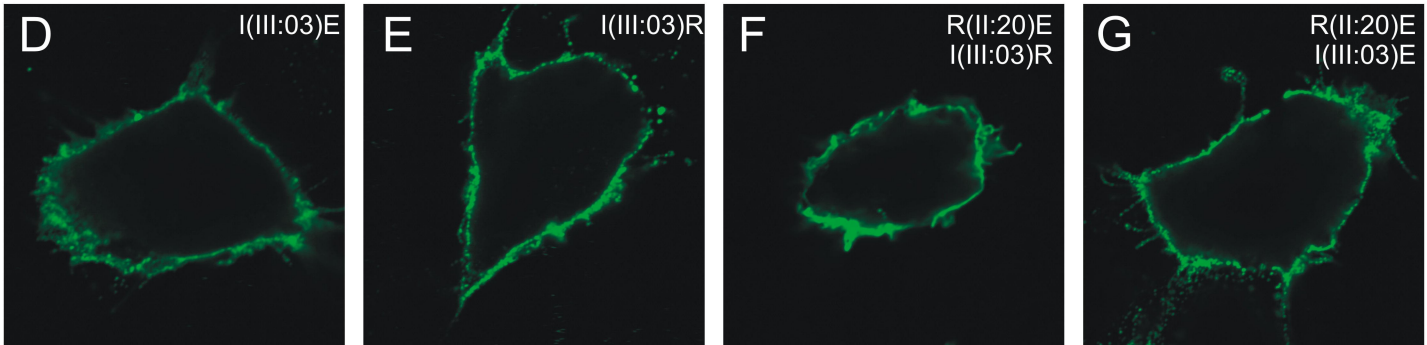
D
I(III:03)E
E
I(III:03)R
F
R(II:20)E
I(III:03)R
G
R(II:20)E
I(III:03)E

Figure 8

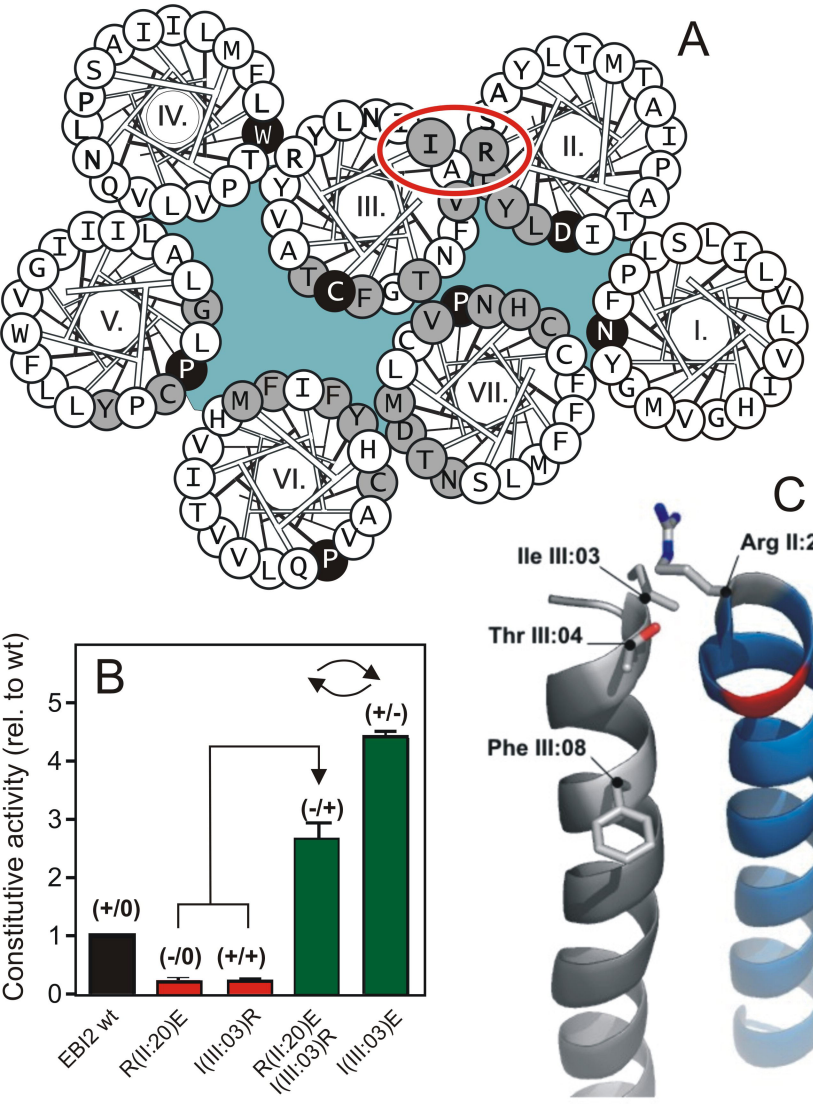
A
IV.
III.
II.
V.
I.
VI.
VII.
I
R
C
P
D
N
W
T
L
B
Constitutive activity (rel. to wt)
0
1
2
3
4
5
(+/0)
(-/0)
(+/+)
(-/+)
(+/-)
EBI2 wt
R(II:20)E
I(III:03)R
R(II:20)E
I(III:03)R
I(III:03)E
C
Ile III:03
Arg II:20
Thr III:04
Phe III:08

Figure 9

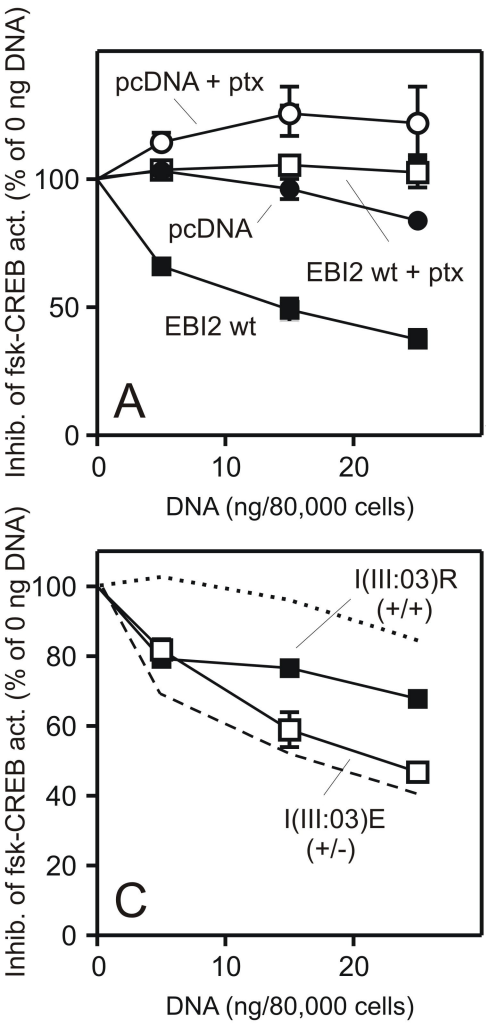
pcDNA + ptx
pcDNA
EBI2 wt + ptx
EBI2 wt
A
Inhib. of fsk-CREB act. (% of 0 ng DNA)
DNA (ng/80,000 cells)

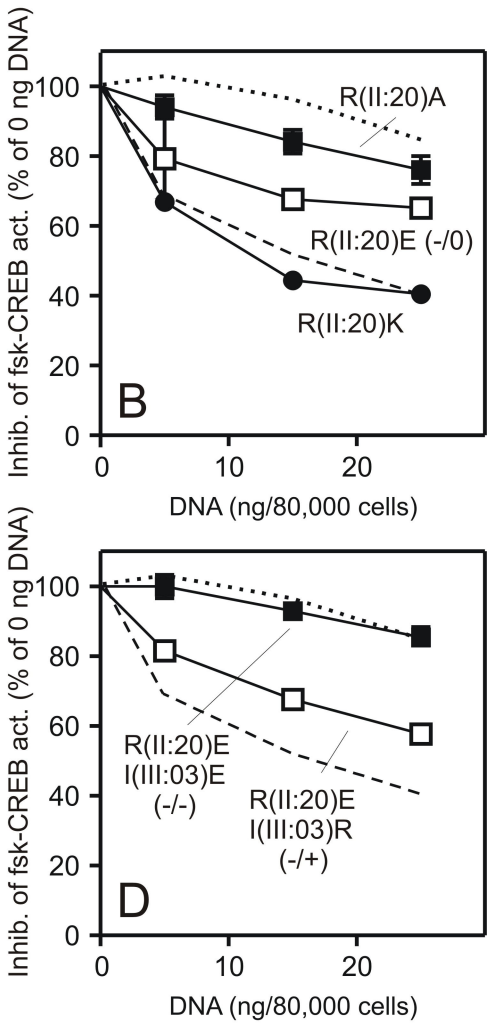
R(II:20)A
R(II:20)E (-/0)
R(II:20)K
B
Inhib. of fsk-CREB act. (% of 0 ng DNA)
DNA (ng/80,000 cells)

I(III:03)R
(+/+)
I(III:03)E
(+/-)
C
Inhib. of fsk-CREB act. (% of 0 ng DNA)
DNA (ng/80,000 cells)

R(II:20)E
I(III:03)E
(-/-)
R(II:20)E
I(III:03)R
(-/+)
D
Inhib. of fsk-CREB act. (% of 0 ng DNA)
DNA (ng/80,000 cells)

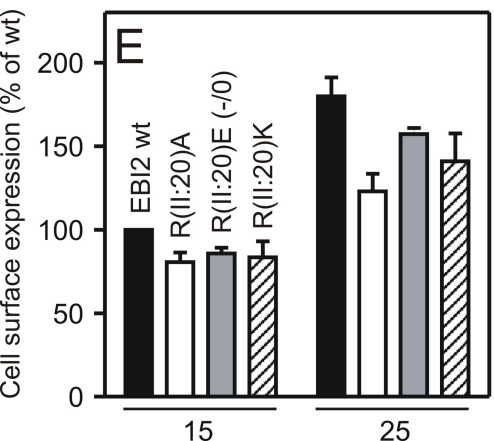
EBI2 wt
R(II:20)A
R(II:20)E (-/0)
R(II:20)K
E
Cell surface expression (% of wt)
15
25

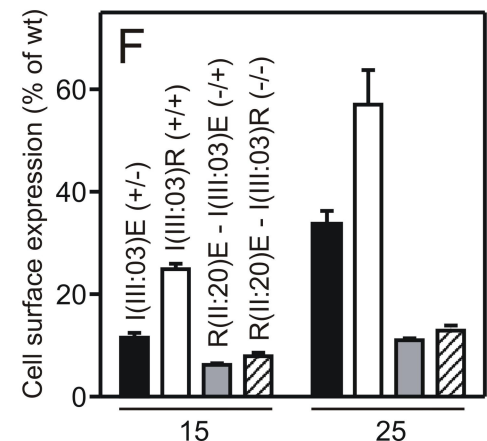
I(III:03)E (+/-)
I(III:03)R (+/+)
R(II:20)E - I(III:03)E (-/+)
R(II:20)E - I(III:03)R (-/-)
F
Cell surface expression (% of wt)
15
25